nature plants

SUPPLEMENTARY INFORMATION
https://doi.org/10.1038/s41477-018-0263-1

In the format provided by the authors and unedited.

# Decreases in global beer supply due to extreme drought and heat

**Wei Xie[1*], Wei Xiong[2,3,4], Jie Pan[2], Tariq Ali[1], Qi Cui[5], Dabo Guan[6,7*], Jing Meng[8], Nathaniel D. Mueller[9], Erda Lin[2*] and Steven J. Davis[9,10]**

[1]China Center for Agricultural Policy, School of Advanced Agricultural Sciences, Peking University, Beijing, China. [2]Institute of Environment and Sustainable Development in Agriculture, Chinese Academy of Agricultural Sciences, Beijing, China. [3]International Maize and Wheat Improvement Center, Texcoco, Mexico. [4]College of Agronomy, Henan Agricultural University, Zhengzhou, Henan, China. [5]School of Economics and Resource Management, Beijing Normal University, Beijing, China. [6]Department of Earth System Science, Tsinghua University, Beijing, China. [7]School of International Development, University of East Anglia, Norwich, UK. [8]Department of Politics and International Studies, University of Cambridge, Cambridge, UK. [9]Department of Earth System Science, University of California, Irvine, CA, USA. [10]Department of Civil and Environmental Engineering, University of California, Irvine, CA, USA.
*e-mail: xiewei.ccap@pku.edu.cn; dabo.guan@uea.ac.uk; linerda@caas.cn

# Decreases in global beer supply due to extreme drought and heat

Wei Xie[1*], Wei Xiong[2,3,4], Jie Pan[2], Tariq Ali[1], Qi Cui[5], Dabo Guan[6,7*], Jing Meng[8], Nathaniel D. Mueller[9], Erda Lin[2*], and Steven J. Davis[9,10]

[1] China Center for Agricultural Policy, School of Advanced Agricultural Sciences, Peking University, Beijing, China

[2] Institute of Environment and Sustainable Development in Agriculture, Chinese Academy of Agricultural Sciences, Beijing, China

[3] International Maize and Wheat Improvement Center, Texcoco, Mexico

[4] College of Agronomy, Henan Agricultural University, Zhengzhou, Henan, China

[5] School of Economics and Resource Management, Beijing Normal University, Beijing, China

[6] Department of Earth System Science, Tsinghua University, Beijing, China

[7] School of International Development, University of East Anglia, Norwich, UK

[8] Department of Politics and International Studies, University of Cambridge, Cambridge, UK

[9] Department of Earth System Science, University of California, Irvine, CA, USA

[10] Department of Civil and Environmental Engineering, University of California, Irvine, CA, USA

* Correspondence to Wei Xie (xiewei.ccap@pku.edu.cn) or Dabo Guan (dabo.guan@uea.ac.uk) or Erda Lin (linerda@caas.cn).

## Supplementary Information

## 1. Background

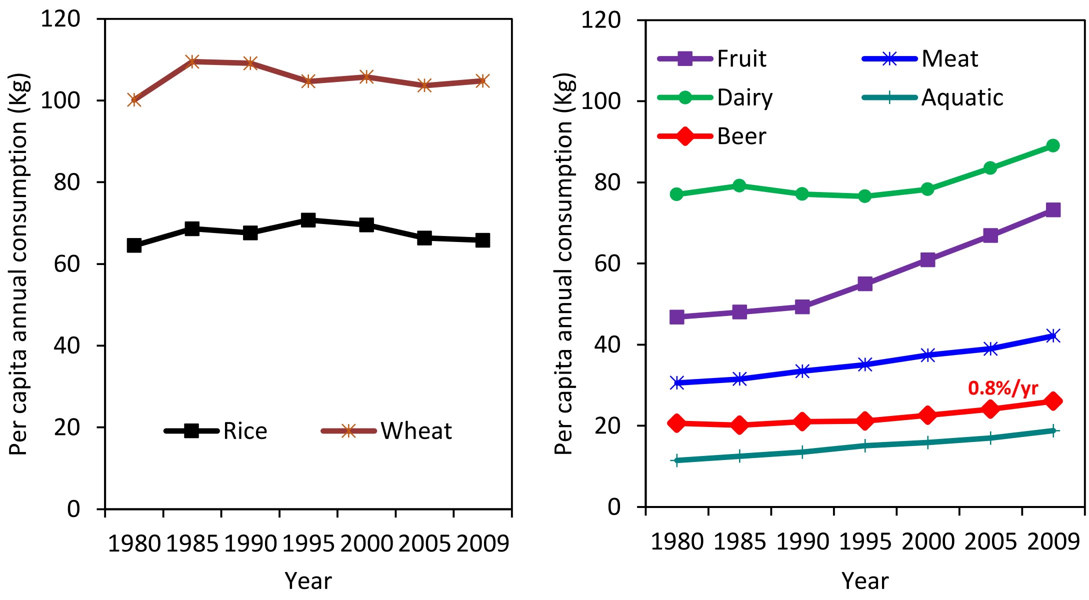


**Figure SI-1. Global food consumption (kg/capita/year)[1]**

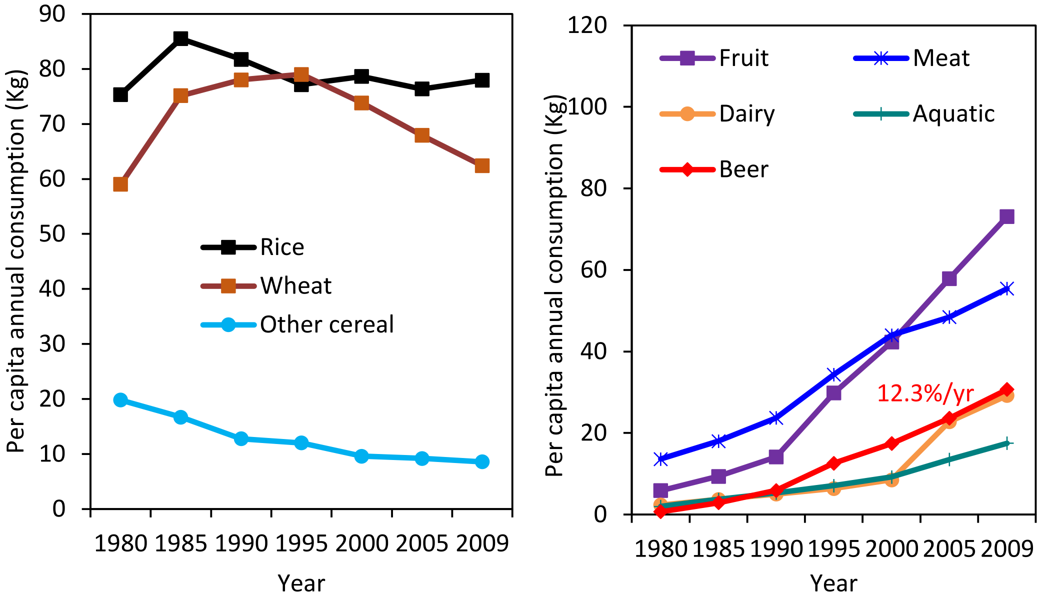


**Figure SI-2. Food consumption in China (kg/capita/year)[1]**

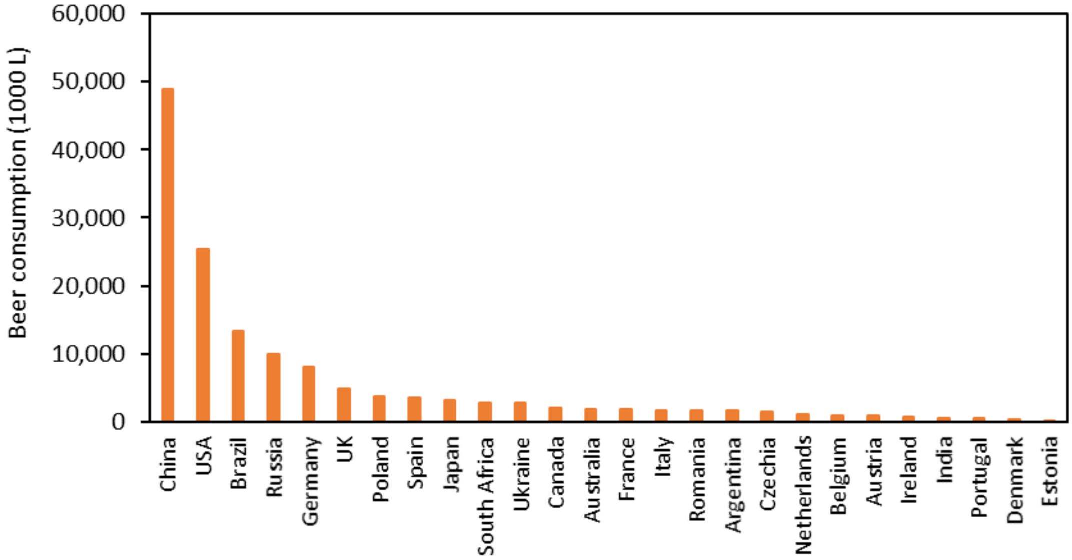


**Figure SI-3. Annual total beer consumption by country in 2011 (1000L)[1]** . Here are the selected main beer consumption countries. In this study, we focused on those countries having one or more of significant barley or beer production, consumption or trade, both in total and per capita terms; for other counties, we aggregated as the rest of the corresponding continents.

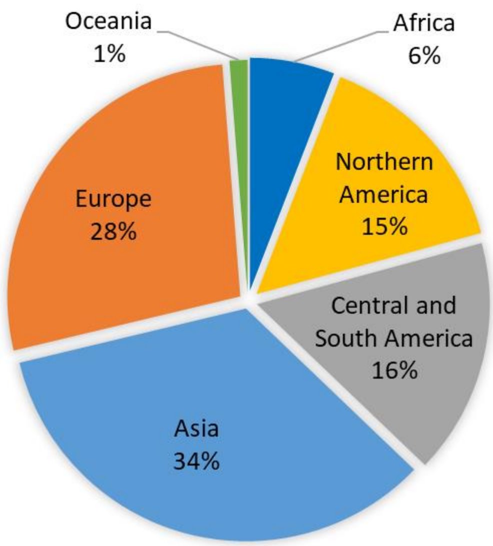


**Figure SI-4. Regional comparison of beer consumption (% shares in 2011)[1]**

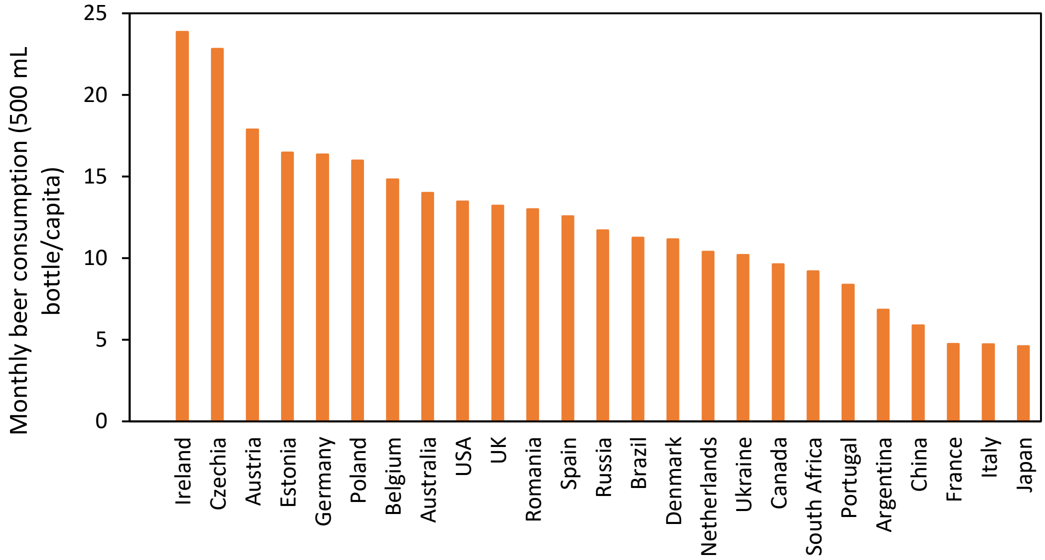


**Figure SI-5. Monthly beer consumption per capita by country in 2011 (500 mL bottle/capita)[1]**. Here are the selected main beer consumption countries. In this study, we focused on those countries having one or more of significant barley or beer production, consumption or trade, both in total and per capita terms; for other counties, we aggregated as the rest of the corresponding continents.

## 2. Methods and Data

### 2.1 Overall framework

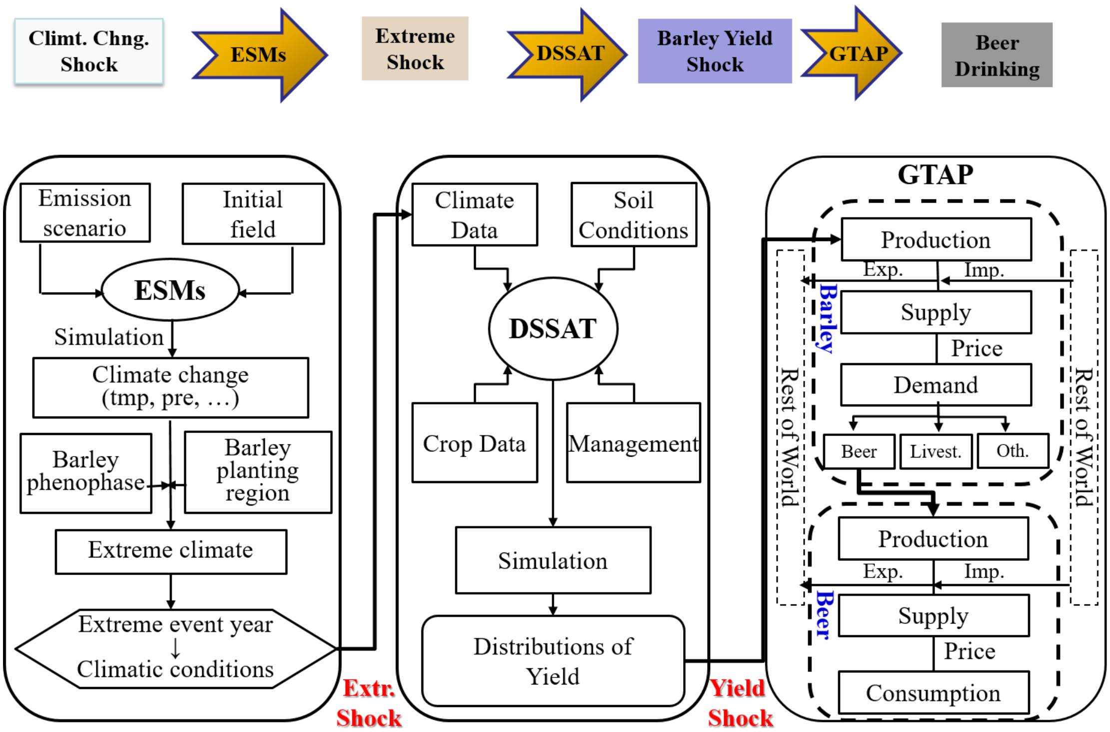


**Figure SI-6. The linkage of ESM-DSSAT-GTAP models**

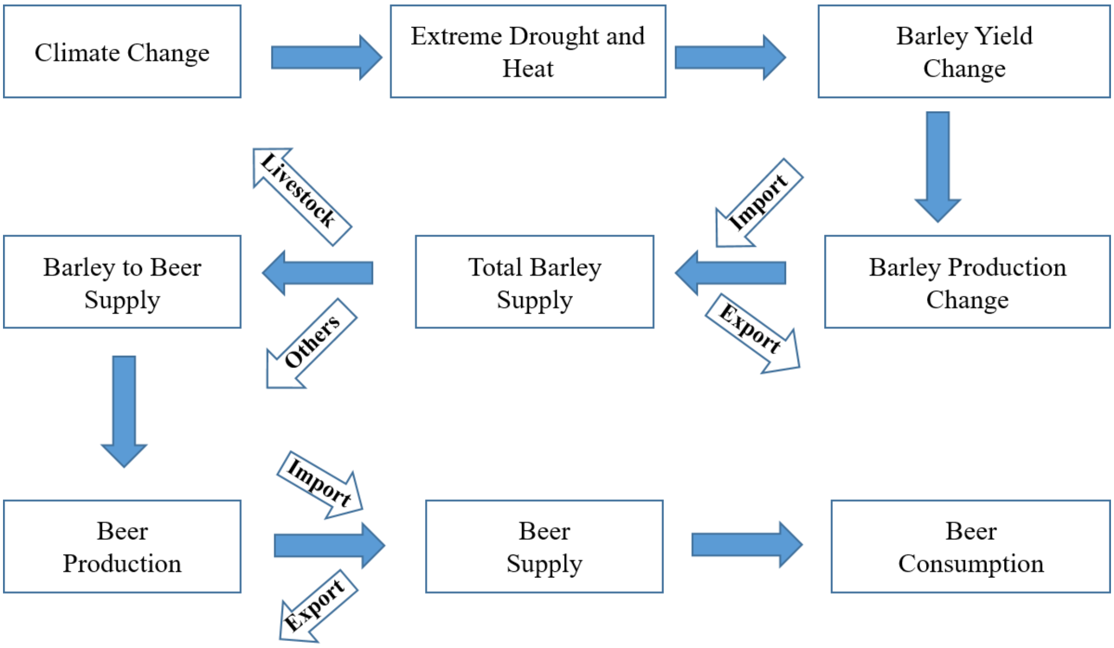


**Figure SI-7. Transmission process of climate change to beer consumption**

### 2.2 Earth System Models (ESMs)

Fig. SI-8 diagrams our selection of extreme event years using ESMs. First, we used historical data (1981-2010) to calculate global indices of extreme drought (based on the standard precipitation index, *SPI*) and extreme heat (based on extreme degree days 30°C+, *EDD*). We then determined the thresholds for 100-year global drought and heat events ($DI^{100}$ and $HI^{100}$), and estimated future global SPI and EDD values under 5 ESMs (GFDL-ESM2M, HadGEM2-ES, IPSL-CM5A-LR, MIROC-ESM-CHEM, NorESM1-M) for each of 4 RCP scenarios (RCP2.6, RCP4.5, RCP6.0, RCP8.5). Finally, we identified modeled "extreme event years" as years with concurrent drought and heat (i) during barley growing season and (ii) in areas where barley is now grown which are (iii) more severe than 100-year events in the historical record (as a weighted average of the barley-growing grid cells).

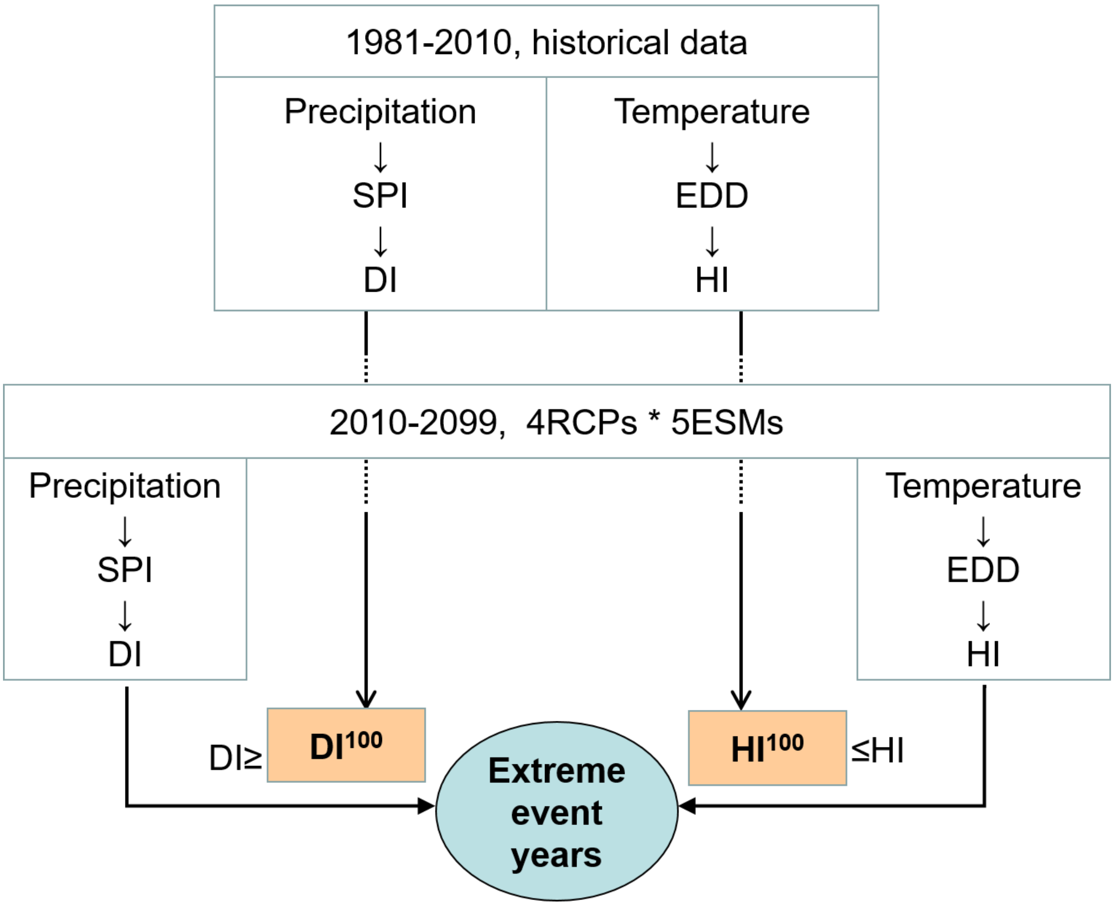


**Figure SI-8. Flowchart of selecting extreme event years during 2010-2099**

#### 1) Global barley drought events threshold value

First, the standardized precipitation index (*SPI*)[2] is calculated using historical daily precipitation (unit: mm) during the barley growing season for each grid cell in global barley planting regions over the period 1981-2010. Here, the growing season is defined as the duration between planting and harvest dates for each grid cell (the data for these dates is from Sacks et al, 2010[3]). Historical daily weather data from 1981-2010 come from the AgMERRA dataset[4]. The AgMERRA is a post-processing of the NASA Modern-Era Retrospective Analysis for Research and Applications (MERRA) suitable for agricultural modeling, featuring consistent, daily time series data and the data demonstrates a similar pattern to other observed historical products, and also substantially improves the representation of daily precipitation distributions of extreme events[4].

Next, an annual global barley drought index is calculated by the following equation:

$$DI_y = \sum_{g=1}^{n} A_g \times SPI_{g,y} \text{ , when } SPI_{g,y} \leq -1.0 \quad (1)$$

where $DI_y$ is global barley drought index for year *y*; $A_g$ is the scaling factor equal to the ratio of the area for grid cell '*g*' to total area in global barley planting region; $SPI_{g,y}$ is the standardized precipitation index for grid cell '*g*' and year '*y*'; *n* is the total number of grid cells for planting barley.

Finally, we fit the annual global barley drought indices with Pearson-III distributions (the "best" universal model for describing probability distribution of extreme events [5]), and use the fitted curves to derive the global barley drought index $DI^{100}$ corresponding to a 1 in 100 year probability:

$$f(x) = \begin{cases} \frac{\beta^{\alpha}}{\Gamma(\alpha)}(x-a)^{\alpha-1}e^{-\beta(x-a)}, & when\ x > a \\ 0, & when\ x < a \end{cases} \quad (2)$$

$$p = \int_{x_p}^{\infty} \frac{\beta^{\alpha}}{\Gamma(a)}(x-a)^{\alpha-1}e^{-\beta(x-a)}dx \quad (3)$$

where *α* is shape parameter, *β* is scale parameter, *a* is location parameter, *x* is annual global barley drought index, *p* is probability and *xp* is the drought event threshold value when probability is set to *p* ($DI^{100}=Xp$ when *p*=1/100).

**2) Global barley heat events threshold value**

Extreme heat can influence crop growth via both direct heat stress and by increasing evaporative demand, thus depleting soil moisture and subsequently reducing carbon assimilation[6-7]. We calculate extreme degree days in exceedance of 30°C (*EDD*) as an index of extreme heat exposure. EDD are calculated using AgMERRA daily maximum and minimum surface temperature for each grid cell and each year across global barley planting regions during the barley growing season from 1981-2010. The EDD temperature threshold (30°C) is in accord with the existing literature that temperature exposure in excess of 30°C will be harmful to the growth of barley [8-10].

$$EDD_{g,y} = \sum_{i=1}^{d_g}(T_{g,y,i} - 30) \text{ , when } T_{g,y,i} \geq 30°\text{C} \quad (4)$$

where $EDD_{g,y}$ is extreme degree days for grid cell *g* and year *y;* $T_{g,y,i}$ is daily mean surface temperature in day *i* for grid cell *g* and year *y*; *dg* is the number of days in growing season for grid cell *g*.

Annual global barley heat index is then calculated as:

$$HI_y = \sum_{g=1}^{n} A_g \times EDD_{g,y} \quad (5)$$

where $HI_y$ is the global barley heat index; $A_g$ is the scaling factor equal to the ratio of the area for grid cell '*g*' to total area in global barley planting region; *n* is the total number of grid cells for planting barley.

Finally, using the similar method to derive global barley drought events threshold value in equation (2) and (3), the global barley heat events threshold value ($HI^{100}$) is derived.

To verify whether the Pearson III distribution adequately fits our distributions, we also performed a statistical test. We use the Kolmogorov-Smirnov (K-S) test to compare the ECDF (Empirical Cumulative Distribution Function) of extreme drought and heat indices with the Pearson III CDF (Fig. SI-9). The K-S test found that the value of $D_{max}$=10.95 for drought and 4.48 for heat index, respectively (with sample size of 30 - historical data from 1981-2010). These values are well below the critical value D (30, 0.05) = 24 at 5% confidence level. The test fails to reject the null hypothesis that the sample is drawn from a Pearson III distribution, leading us to conclude that it is reasonable to use Pearson III distribution to fit the sample.

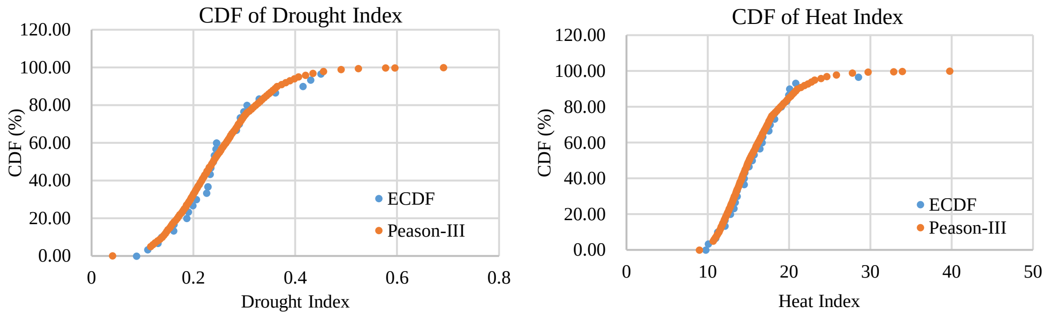


**Figure SI-9. Comparison of the empirical cumulative distribution Function of extreme drought and heat indices (n=30 years) with the Pearson III CDF**

**3) Global barley drought index (*DIy*) for 4 RCPs and 5 ESMs**

*Global barely drought index* ($DI_y$, where *y* represents year) in future years are projected by equation (1) using global climate scenarios data from 2010-2099. The climate scenarios data were extracted from output archives of five ESMs under four RCPs (RCP2.6, RCP4.5, RCP6.0, RCP8.5) retrieved from CMIP website. The data were interpolated into 0.5°x0.5° horizontal resolution and bias-corrected with respect to historical observation by Hempel et al.[11] to remove systematic errors.

**4) Global barley heat index ($HI_y$) for 4 RCPs and 5 ESMs**

The global barley heat index ($HI_y$) was calculated similar to the global barley drought index (section 3), but using equations (4) and (5).

**5) Global integrated extreme event index (*EEIy*)**

As shown in Fig. SI-10, the value of global drought/heat index of historical data is taken as threshold $DI^{100}/HI^{100}$ when their respective frequency is equal to 1%. When the global drought/heat index $DI_y/HI_y$ of climate model is greater than or equal to the threshold, the corresponding model year (all the dots towards right side of the green vertical line in Figure SI-10) is defined as extreme drought/heat year. We define “extreme event years” as years with concurrent drought and heat (i) during barley growing season and (ii) in areas where barley is now grown which are (iii) more severe than 100-year events in the historical record (as a weighted average of the barley-growing grid cells). So we select global extreme event years when both global extreme drought ($DI_y \geqslant DI^{100}$) and global extreme heat ($HI_y \geqslant HI^{100}$) concurrently strike in the same year. This situation can occur either in the form of concurrent heat and drought or as one following the other. Then we calculate a global integrated extreme event index ($EEI_y$) for the selected years based on the following equation:

$$EEI_y = \begin{cases} \dfrac{DI_y - DI^{100}}{DI^{100}} + \dfrac{HI_y - HI^{100}}{HI^{100}}, & when \;\; DI_y \geq DI^{100} \;\; and \;\; HI_y \geq HI^{100} \\ -1, & when \;\; DI_y < DI^{100} \;\; or \;\; HI_y < HI^{100} \end{cases} \quad (6)$$

All the modeled extreme event years where $EEI_y \geq 0$ are selected to simulate global barley yield using the crop model and subsequently beer supply and price using the economic model.

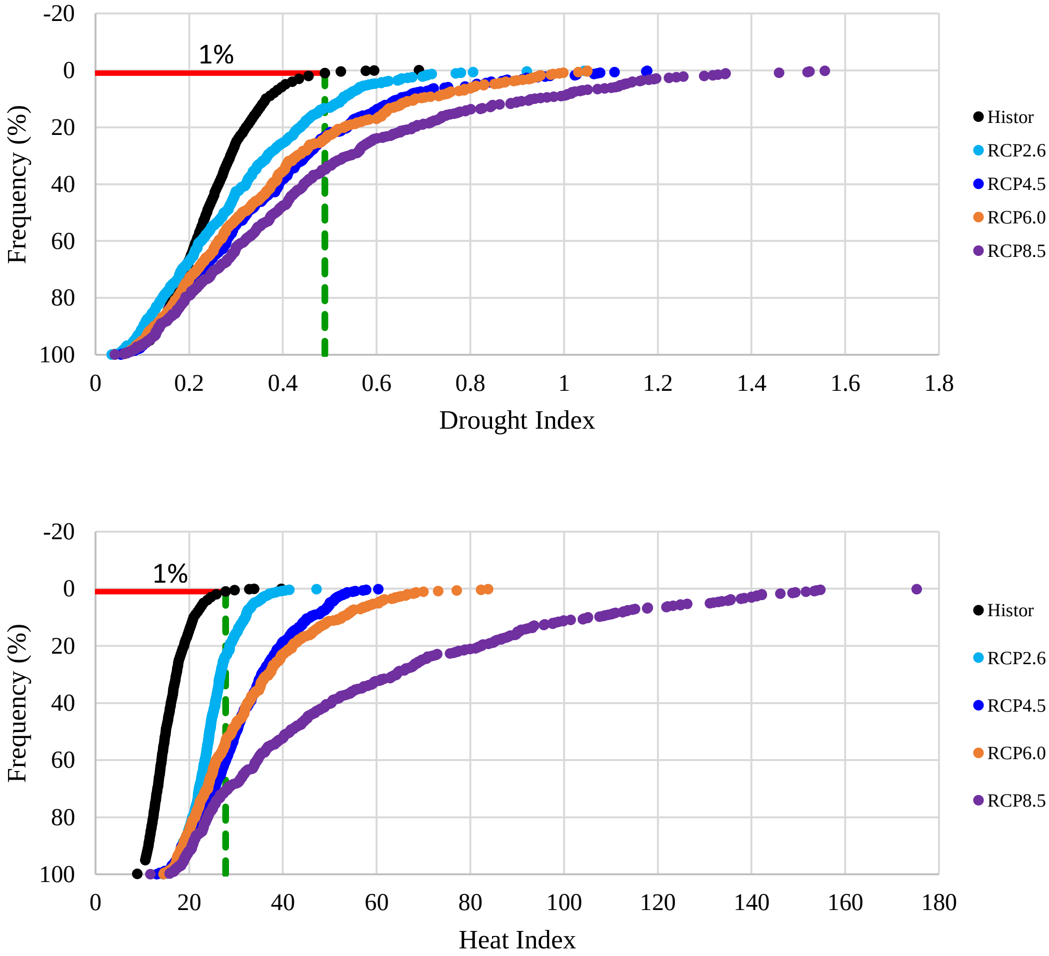


**Figure SI-10. Frequency of historical and simulated global drought (top) and heat (below) index**

## 2.3 Crop model (DSSAT)

The Decision Support System for Agrotechnology Transfer (DSSAT) is a software application program that comprises crop simulation models for over 40 crops. It was developed through the International Benchmark Sites Network for Agrotechnological Transfer (IBSNAT) in the 1980s, with the first release in 1989. The crop simulation models in DSSAT simulate growth, development and yield as a function of the soil-plant-atmosphere dynamics, and they have been used for many applications ranging from on-farm and precision management to regional assessments of the impacts of climate variability and climate change[12, 13]. DSSAT-Barley has been tested in various environments around the globe. For example, barley-specific analyses using DSSAT were performed in Czech Republic which shows that the coefficient of determination between simulated and experimental yields equals 0.88[14]; Other applications in Argentine, Central Europe, Ireland and West Asia all provided the reliability of CERES-Barley in different environments with root-mean-square-error (RMSE) for yield less than 15%[15-18]. A Europe-focused model intercomparison also shows that yields projected by the DSSAT model are near the mean of nine crop models[19].

DSSAT is a site-specific model, requiring explicit inputs of crop genotype, management, climate and soil information[20], therefore we adapted the model into a parallel and spatial application on a High Performance Computer (HPC) by linking the model with geospatial datasets (raster) of climate, soil, and management. Geospatial data of crop calendar, management, and reported yield/area are resampled into the same resolution of 0.5°x0.5° as the simulation cell by a bilinear interpolation method. Initial inputs for running the model in each grid cell include sowing date (the midpoint of reported sowing window)[3], amount and date of fertilizer application, soil profile, daily climate, and cultivars. Nitrogen is applied twice at sowing (60%) and 60 days after sowing (40%) with a sum equaling to value in nitrogen raster in Elliott et al. (2014a, 2014b)[21,22], which includes chemical fertilizer inputs from the Mueller et al. (2012) dataset[23]. Phosphorus and potash are assumed unlimited for the crop in face of the limitation of the model to simulate such effects[24, 25] and lack of explicit nutrient pool information related to P and K in the harmonized world soil database[26].

Spatial information related to crop genotype is unknown so far for the globe so that we conduct an improved spatial calibration procedure to estimate the values for each barley grid[27-29]. We adopted the barley genetic parameters of specific cultivar from pervious works such as Trnka et al., (2004)[14] as the initial parameters. But applying parameters of a few specific cultivars to the whole world is more complicated than it seems, for example, cultivars from Europe may not able to germinate in tropical and semi-tropic conditions and vice versa. Given the lack of observations on the geographic distribution of cultivar traits, this calibration procedure is conducted for every barley grid at no water limitation conditions by sequentially varying 6 genotype parameters to match reported phenology (day to maturity, estimated from calendar raster) and final yield (irrigated yield, extracted from SPAM [30]). A combination of three phenology parameters (P1V: Days to vernalization under optimum vernalizing temperature, P1D: Photoperiod response, P5: Grain filling phase duration) determines the crop maturity period, and a combination of three yield component parameters (G1: Kernel number under optimum conditions, G2: Standard kernel size under optimum conditions, and G3: non-stressed mature tiller weight) defines the biomass yield. The purpose of this parameterization is to identify appropriate cultivars (which may not be a real cultivar) that fit the specific real-world environments, such as a local cultivar that has reasonable growth period to cope with climate stress and match local crop calendar and management. Importantly, this parameterization increased the spatial agreement between simulated and observed maturity day and yield.

There are three types of barley grown worldwide – spring barley, winter barley and alternative barley, but quality requirements for brewing industry are best met by spring varieties, therefore spring barley is the most common type used for brewing[31]. We, therefore, assumed that spring barley is the default type in our simulations. For countries that only have winter barley, such as Austria, we simulated winter barley. For countries that have a mix of spring and winter barley types, mostly in central European regions between 43˚and 53˚north, we conducted two simulations for both spring and winter types, but extracted yield of winter barley only if it exceeded spring barley yield by more than 200%. Area for winter and spring barley for major countries is based on World Agricultural Outlook Board (1994)[32]. Sowing and harvesting dates for spring and winter barley were from Sacks et al., 2010[3].

The DSSAT simulation is conducted for all grids under two water regimes – fully irrigated and no irrigation. For fully irrigated conditions, sowing is defined during the midpoint of sowing window, and irrigation (20mm) is triggered whenever soil water content is less than 80% of the soil water holding capacity. Automatic sowing is applied for no-irrigation barley, when accumulated rainfall in any continuous three days during the sowing window is greater than 25mm, otherwise the first day after the window is applied. Performance of the global spatial simulation is reasonable, as evaluated by comparison between simulated and reported historical yields (1981-2010) at grid, global, and national levels (Figs. SI-17-19). In which global and national simulated yields are aggregated as below:

$$Y_{a,j} = \sum_{i=1}^{n} (Yb_{a,i} \times Ab_i + Yg_{a,i} \times Ag_{a,j}) / \sum_{i=1}^{n} (Ab_{a,i} + Ag_{a,i}) \quad (7)$$

Where $Y_{a,j}$ indicates the simulated yield of country/region *j* during year *a*. *Yb* and *Ab* are simulated irrigated yield and reported irrigated area, while *Yg* and *Ag* are rainfed yield and area. *i* indicated no. of grids and *n* is the number of grids of a country/region or the whole world. Reported yields come from FAOSTAT[1] and are linearly detrended into 1981 technology level.

Future yields are driven by climate scenarios covering the years 2010–2099, with the same settings as historical simulations. $CO_2$ concentration is held constant at 2010 level to isolate the impacts of temperature and precipitation. Yield changes are estimated for extreme event years as the difference between the annual yield and the historical mean yield of 1981–2010.

Despite applying the Global Gridded Crop Model (GGCMs) protocols[33] of the Agricultural Model Intercomparison and Improvement Project[34] and a detailed calibration procedure, projected yield responses can represent uncertainties in the crop model, input data, and parameterization. To date, there is no multi-model simulation experiment at the global scale for barley. Previous multi-model comparisons for staple crops (including wheat and maize) demonstrated that calibration on specific parameters and the use of harmonized geospatial datasets effectively reduced the range among models in terms of the estimated yield response to global warming, and that the DSSAT model produced yield changes that were close to the average of all projections[33,35,36]. Nevertheless, yield damages due to extreme climate events estimated here will undoubtedly differ to some degree from those produced by other models. Future work should produce multi-model comparisons of climate change impacts for barley, and consider the role of other stresses, e.g. phosphorus, potassium, and soil quality.

## 2.4 Global economic model (GTAP)

The barley yield changes from the crop model are used to carry out simulations using Global Trade Analysis Project (GTAP) model to investigate changes in barley production and the impact on beer production and price. GTAP is a well-known and widely used global general equilibrium economic model developed by the Department of Agricultural Economics at Purdue University[37, 38]. The multi-region and multi-sector model uses an extensive global database focusing on the food and agriculture sector, covering 8 food sectors (including livestock and processed food products) and 14 agricultural sectors (crops or combination of crops). The model assumes cost minimization by producers and utility maximization by consumers. In a competitive market setup, prices adjust until supply and demand of all commodities equalize. Representative consumers of each country or region are modeled as having a non-homothetic Constant Difference of Elasticity (CDE) demand function. On the production side, firms combine intermediate inputs and primary factors (e.g., land, labor, and capital) to produce commodities with constant-return-to-scale technology. Intermediate inputs are composites of domestic and foreign components, with the foreign component differentiated by region of origin (the Armington assumption). The model and database have been extensively used in studies of climate change, food security policy, energy, poverty and migration, etc.

Here we use a comparative static analysis approach to simulate the impact of climate changes on beer supply and prices under current economic conditions. In this first study, our aims is to isolate the effects of climate and extreme events rather than those of the socioeconomic preferences. Furthermore, we believe that our focus on extreme events justifies a lack of such scenarios because such events can occur in any year (although with different probability). It would also be challenging to estimate, present, and discuss effects that are sensitive to highly uncertain trajectories of the global economy and dietary preferences, especially for small economic sectors. For example, there is no global study (that we know of) which predicts the future levels of beer consumptions due to changes in income and culture in different countries. We also note that a number of other prominent climate impacts studies[39,40] have used a similar method to project the influence of climate, holding socioeconomic conditions constant. Since current observations of the economy are well understood and widely agreed on, these studies use current values for clarity. The advantage of this method, as demonstrated by the prior studies, is that it avoids the inclusion of future scenarios on population and economic growth that would require many more assumptions and would therefore substantially complicate the interpretation of the results. In particular, it would be difficult to understand the contribution of climate change alone. As constructed, our study describes the impacts on beer supply and price if an extreme event were to occur this year.

To update the GTAP model for the purposes of our study, we split barley and beer from the original database (latest version 9 of GTAP database), design an appropriate sectoral and regional aggregation (34x19 i.e. country/region x sectors, see Appendix Table A1) scheme to the original database (140x57 i.e. country/region x sectors) and introduce some behavioral changes into the standard GTAP model to consider the short run situation after extreme events as follows:

First, we improved the database by splitting barley and beer from the existing sectors, following similar work using GTAP [41-43]. Barely was split from the "other grains" sector and beer from the "beverage and tobacco" sector using the routines from the Splitcom method[44]. In this procedure, the old flows of data at national level are allocated between the new flows using weights. The national weights include the division of each unsplit user's use of the original split commodity among the new commodities; the division of unsplit inputs to the original industry between the new industries; the splitting of new industry's use of each new commodity.

Specifically, barley use is mainly shared between feed, food, processing and others (seed, waste, etc.) [1]. In our process, we assume that processing is mainly covered by beer production, so we allocate all the "processing" share of barley as input to beer sector. The values for barley to different users shown in Table SI-1 are mainly from FAOSTAT[1]. However, we performed a sensitivity analysis for these shares in section 3.6 to reflect the technology change (the possibility of producing more/less beer using the same quantity of barley input) in future. The newly created beer sector is allocated to wholesalers/retailors, restaurants/bars and private household consumption (we got the beer consumed by "food" and other sectors from FAOSTAT[1]). Then the proportion of beer used by "food" sector was allocated to three sectors i.e. "wholesalers/ retailors, restaurants/bars and private household consumption" based on the respective share of the original "b_t" sector by these three sectors. The "own use" (defined as self-use of a sector of its own output, e.g., seed used to sow "barley" or electricity used by the "electricity" sector) of barely was taken from the "seed"; for beer the own use was kept to zero as beer doesn't have self-use. Moreover, we have covered only barley-based beer in our "beer" sector, while the beer produced from other feedstocks (wheat, corn etc.) are placed under "otherbt" sector. Trade shares allocate the original slice of the split commodity into the new commodity for all elements of basic price value, tax, and margin. The trade shares matrix was calculated based on the data from UN Comtrade Database[45].We finally used the RAS method for balancing the newly created database.

**Table SI-1. Barley domestic use ratio (%)**

| Country | Beer | Feed | Food | Seed/ Other utility |
|---|---|---|---|---|
| Australia | 8.5 | 89.0 | 0.0 | 2.5 |
| Rest of Oceania | 13.9 | 82.1 | 0.3 | 3.7 |
| China | 74.1 | 17.1 | 6.5 | 2.3 |
| Japan | 29.3 | 60.3 | 4.5 | 5.9 |
| Rest of Asia | 4.1 | 82.9 | 1.5 | 11.6 |
| India | 7.4 | 9.5 | 77.4 | 5.7 |
| Canada | 11.9 | 79.9 | 0.1 | 8.2 |
| United States of America | 74.0 | 19.5 | 3.9 | 2.6 |
| Rest of North America | 72.2 | 23.0 | 0.0 | 4.8 |
| Argentina | 42.7 | 20.1 | 0.0 | 37.2 |
| Brazil | 82.8 | 5.5 | 0.0 | 11.7 |
| Rest of South America | 48.2 | 17.5 | 18.6 | 15.7 |
| Rest of America | 61.9 | 3.1 | 1.4 | 33.7 |
| Austria | 19.5 | 75.4 | 0.2 | 4.9 |
| Belgium | 27.6 | 69.6 | 0.1 | 2.7 |
| Czech Republic | 35.5 | 59.8 | 0.3 | 4.4 |
| Denmark | 5.0 | 81.9 | 0.0 | 13.2 |
| Estonia | 17.0 | 77.2 | 1.8 | 4.0 |
| France | 2.6 | 91.0 | 0.3 | 6.1 |
| Germany | 19.3 | 77.3 | 0.2 | 3.2 |
| Ireland | 13.5 | 83.2 | 0.1 | 3.2 |
| Italy | 18.5 | 79.2 | 1.6 | 0.7 |
| Netherlands | 22.5 | 73.4 | 0.8 | 3.2 |
| Poland | 20.7 | 68.9 | 6.6 | 3.8 |
| Portugal | 36.1 | 59.3 | 2.7 | 1.9 |
| Spain | 8.5 | 90.4 | 0.1 | 1.1 |
| United Kingdom | 30.1 | 67.2 | 0.9 | 1.8 |
| Rest of EFTA | 14.2 | 76.1 | 3.9 | 5.8 |
| Romania | 46.7 | 34.8 | 3.5 | 15.1 |
| Russian Federation | 15.2 | 79.8 | 1.1 | 3.8 |
| Ukraine | 8.3 | 72.0 | 1.9 | 17.8 |
| Rest of Europe | 8.2 | 73.2 | 2.0 | 16.6 |
| South Africa | 94.0 | 2.6 | 1.0 | 2.4 |
| Rest of Africa | 12.8 | 28.9 | 40.4 | 17.9 |

Source: FAOSTAT[1].

Regarding the choice of correct parameter values during the split process, we paid extra attention to the consumers' preferences (income elasticity) and consumers' response to price changes (price elasticity) as they are the main factors affecting beer demand. The values for the relevant parameters related to income elasticity and price elasticity for beer in our analysis were carefully selected based on literature[46]. Due to their critical role in beer consumption, we also tested the sensitivity of our results to the choice of the parameter values in section 3.6.

Second, our sectoral aggregation scheme for GTAP ensures that all the competing and complimenting sectors for both barley and beer are present in the most disaggregated form. For example, for barley, other crops compete for inputs of production and both livestock and households on the demand side are kept (see Appendix Table A1). Beer is bought locally by wholesalers/retailors (covered in "Trade" sector), restaurants/bars (covered in "Recreational services" sector), and consumed by private consumers (represented by the default "Private Households"). For regional aggregation, we kept the details for all the countries having one or more of significant barley or beer production, consumption or trade, both in total and per capita terms; for other counties, we aggregated as the rest of the corresponding continents (Appendix Table A2).

Third, the yield shocks for barley were incorporated into GTAP model via changes in land use efficiency for the land used by barley production in each region (parameter "*afe*" in Eq. 8) , the conventional method for translating yield perturbations into economic models [47-49]. Land use efficiency affects both price and demand for land in the following fashion:

*Equation of Price of primary factor composite in each sector/region* (The following equations are in percentage form, same hereafter):

$$pva_{j,r} = \sum_{k=1}^{n}(SVA_{k,j,r} * (pfe_{k,j,r} - afe_{k,j,r})) \quad (8)$$

where

*j* = production commodity (industry); *r* = region; *k* = endowment commodity, the total number of endowment commodity is *n*

$pva$ = firms' price of value added in industry *j* of region *r*

$pfe$ = firms' price for endowment commodity *k* in ind. *j*, region *r*

$SVA$ = share of *k* in total value added in *j* in *r*

$afe$ = primary factor augmenting technology change, specific to each sector of each region

In the improved model, to reflect the difficulty of substitution between land and other key inputs like labor and capital, we surveyed the existing literature in this area. The literature shows that in case of extreme events, it is hard for industrial sectors to substitute land with other key inputs and this phenomenon is reflected by the lower value of the elasticity of substitution between land and the other inputs[50,51]. Therefore, for barely production in the extreme event years, we choose a fraction of the original value for the relevant parameter. Specifically, we changed the elasticity of substitution between endowments (ESUBVA, Eq. 9, and Fig. SI-11) for barely to 10% of original value as suggested in previous vast literature[50,51]. Considering the uncertainty of the key parameters, we have further analysed the sensitivity of the key parameters in section 3.6.

*Endowment commodities' input to each regions/industries*:

$$qfe_{k,j,r} = -afe_{k,j,r} + qva_{j,r} - ESUBVA_j * (pfe_{k,j,r} - afe_{k,j,r} - pva_{j,r}) \quad (9)$$

where

*qfe* = demand for endowment *k* for use in industry *j* in region *r*

*qva* = value added in industry *j* of region *r*

*ESUBVA* = elasticity of substitution between capital/labor/land in certain industry *j*

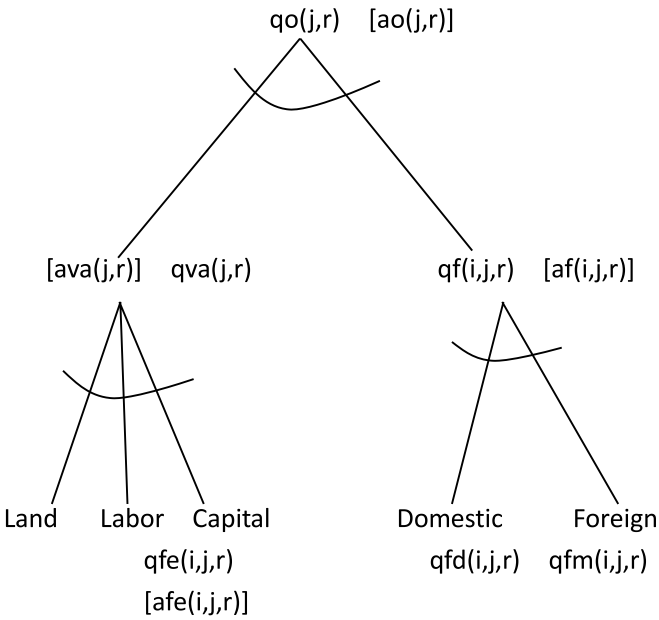


**Figure SI-11. Land input to crops and substitution of land with other endowments (labor, capital)**

In the original GTAP model, capital and labor can freely move between production activities, while for land and natural resources such movement is largely restricted (Eqs. 10, 11; Fig. SI-12). By default, different crops can adjust their demand for land within some margin (with transformation elasticity *ETRAE* = -1). ). However, under the drought and extreme heat conditions of the real world, people may first want to ensure their food security by expanding the area for staple food crops (like wheat) rather than that of barley, resulting in reduced barley planted area. In this study, we made a less severe assumption that land shares will stay unchanged for barley and other competing crops, considering the total supply of land can hardly expand in short time. While we assume that labor, machinery and other inputs to barley (e.g., fertilizers, irrigation, etc.) can be augmented by increasing the working hours or additional investment. So, in our improved model, the acreage of land used for barley (or any other crops) in the normal year is still used for barley (or any other crops) during extreme event years (ETRAE = 0).

*Allocation of the sluggish endowments across sectors:*

$$qoes_{k,j,r} = qo_{k,r} + ETRAE_k * (pm_{k,r} - pmes_{k,j,r}) \qquad (10)$$

where

*qoes* = supply of sluggish endowment *k* used by *j* in *r*

*qo* = industry output of commodity *k* in region *r*

*ETRAE* = Elasticity of transformation for sluggish primary factor endowments (non-positive, by definition)

*pm* = market price of commodity *k* in region *r*

*pmes* = market price of sluggish endowment *k* used by *j* in *r*

*Composite price for sluggish endowments:*

$$pm_{k,r} = \sum_{j=1}^{n}(REVSHR_{k,j,r}) * pmes_{k,j,r} \quad (11)$$

where

*REVSHR* = share of endowment use by different industries

Mobile endowments (capital and labor) were allowed to behave normally as they can be provided via higher investment under the extreme events (Eqs. 12, 13).

*Allocation of the mobile endowments across sectors:*

$$qo_{k,r} = \sum_{j=1}^{n}(SHREM_{k,j,r}) * qfe_{k,j,r} \quad (12)$$

where

*SHREM* = share of mobile endowment *k* used by sector *j* at market prices

*Composite price for mobile endowments:*

$$pm_{k,r} = VFM_{k,j,r}/qfe_{k,j,r} \quad (13)$$

where

*VFM* = Producer expenditure on endowment *k* by industry *j* in *r* valued at market prices

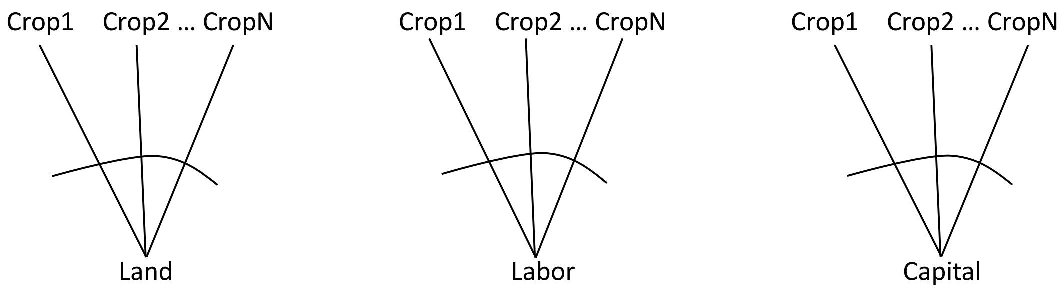


**Figure SI-12. Endowment allocation to different industries/sectors**

We also add the changes in barley's foreign trade to production for each country, thereby simulating the changes in barley supply.

Finally, for simulating the changes in beer supply and prices after experiencing barley production shocks, we consider regional differences in allocation of barley to all users (beer, feed, food and others). In a normal year, barley shares to different users come from FAOSTAT[1] (see SI Table SI-1). In an extreme event year, barley is distributed to different users according to the profit maximization principle. Final beer supply for each country also contains net beer imports.

It is noted that in our GTAP model, we do not consider stockpiling effects. First, barley stocks are historically much lower than staple food crops such as wheat, rice, and maize (e.g., during 1980-2017, the global average ratio of ending-period stocks to prior-year production was 18% for barley, as compared to 30% for wheat, 28% for rice and 25% for maize[52]). Stocks could be increased, but—although barley can be stored—storage of grain intended for beer production requires very specific conditions to preserve its quality for malt extraction. And even then, studies suggest that barley storage reduces barley quality[53,54] and thereby beer quality[55]. Finally, because it won't be possible to predict the year when the extreme event will strike, and it may not be feasible or desirable to manage large stockpiles of barley every year in case an extreme event occurs.

## 2.5 Uncertainty Analysis

Following the general framework designed by Hawkins and Sutton[56], we perform a sensitivity analysis to test the relative importance of different factors to beer supply. We decompose the uncertainty into contributions of “physical shocks” uncertainty, ‘technology’ uncertainty, and “economic behavior” uncertainty. “Physical shocks” uncertainty comes from the physical models and possible barley stockpiling and is performed by varying the size of barley yield shocks; “technology” uncertainty comes from better/worse technology that can lower/increase the amount of barley required to produce the same quantity of beer; “economic behavior” uncertainty is based on the possible changes of beer price elasticity, income elasticity and substitution of land with others inputs for barley production.

Based on our “reported estimation” that refer to the original average impacts on beer consumption during 2010-2099, the uncertainty is identified by changing single input one at a time (with ±10% variation) while holding other inputs at their original values. We loop the procedure for each of the factors, and then compare the sum of these single marginal impacts to the total impacts when all factors are sampled simultaneously. The residual between the total impact and the sum of all single impacts is attributed to “interaction” among sources of uncertainty. Section 3.6 presents the results of uncertainty analysis and along with a discussion of other limitations.

# 3. Supporting results

## 3.1 Severity and frequency of extreme events risk under climate change

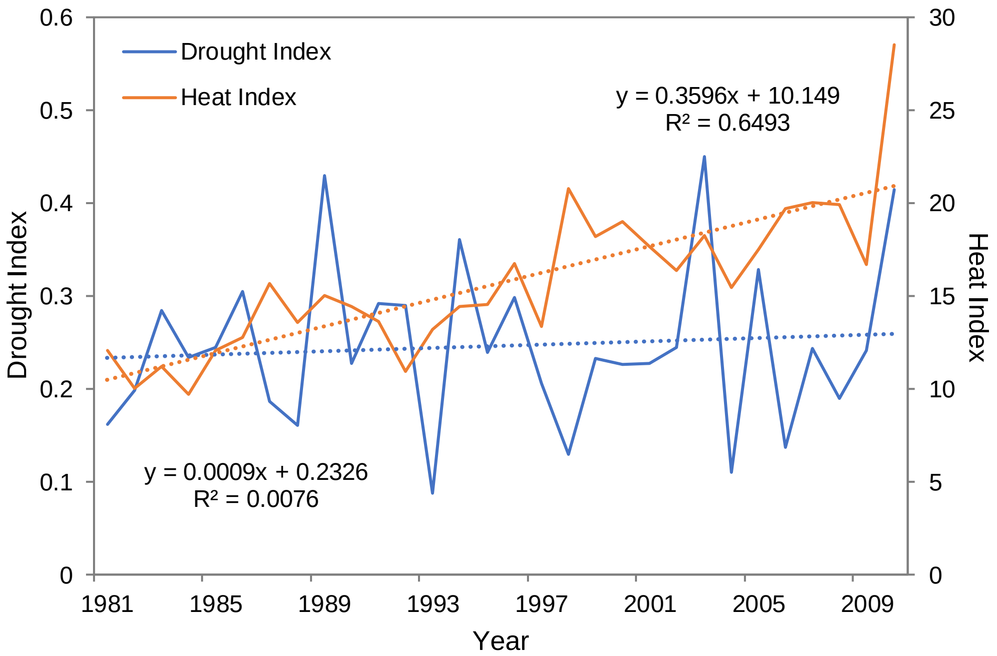


**Figure SI-13. Changes of Drought and Heat Indices in Global Barley Areas from 1981 to 2010.** Dotted lines denote linear trends for each index (n=30 years).

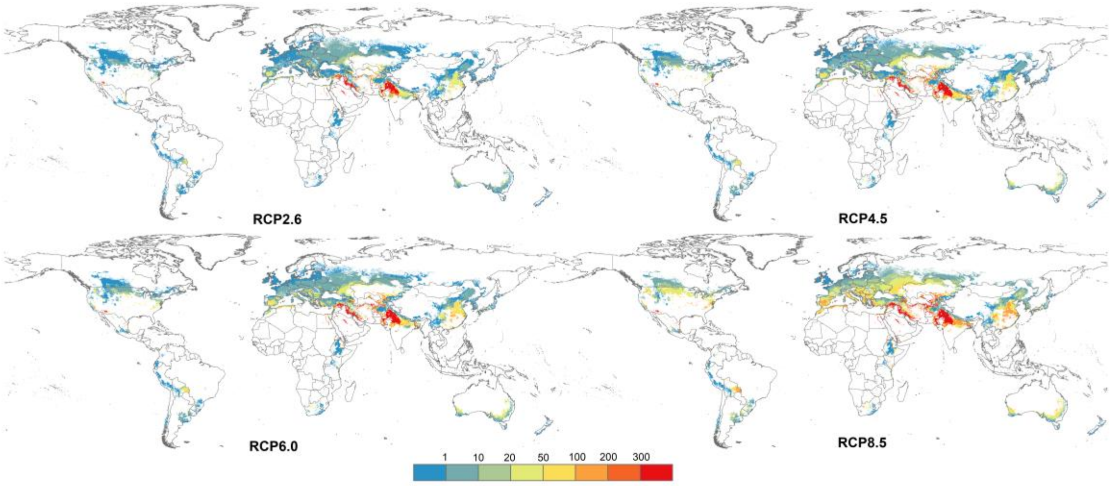


**Figure SI-14. Spatial patterns of EDDs across all extreme event years under the four RCP scenarios.**

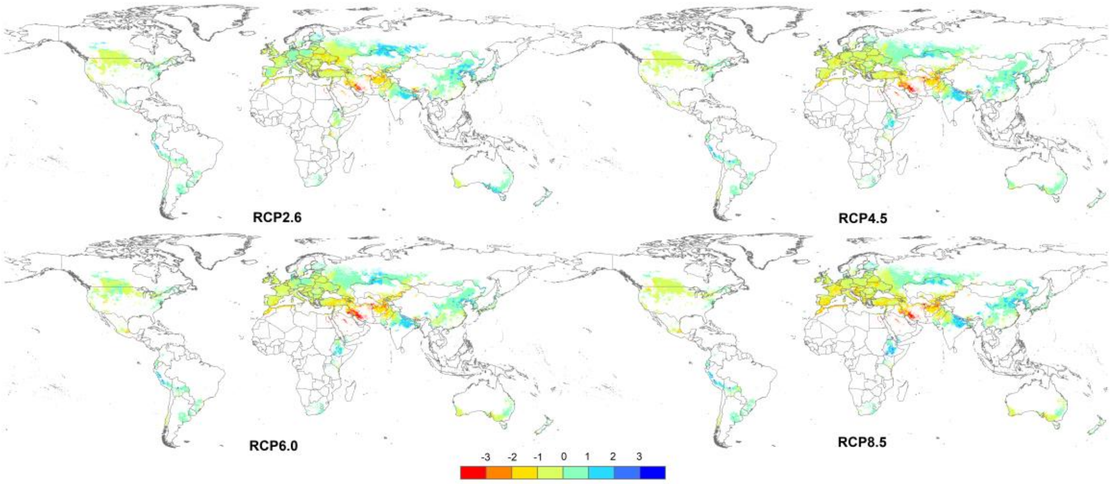


**Figure SI-15. Spatial patterns of SPI across all extreme event years under the four RCP scenarios.**

## 3.2 Impact of the extreme events on barley yield

### 3.2.1 Validation of the simulation results with historical data

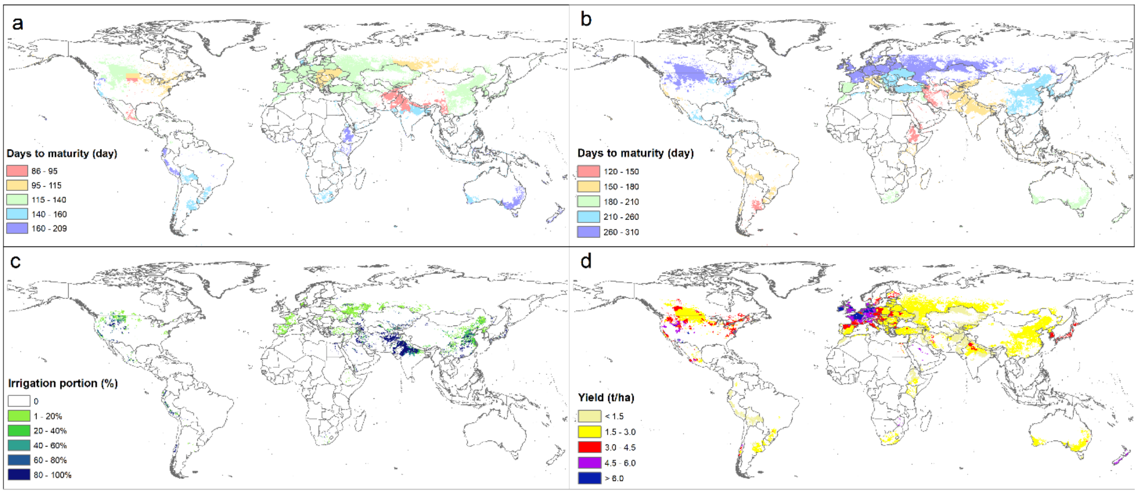


**Figure SI-16. Global gridded barley calendar, irrigation portion, and yield used to parameterize model's cultivar coefficients at grid level. a) days to maturity – spring barley, b) days to maturity – winter barley, c) irrigation proportion, and d) yield.** Global barley days to maturity is obtained from the Center for Sustainability and Global Environment (SAGE), which is the result of digitizing and geo-referencing existing observations of crop planting and harvesting dates[3]. Irrigation portion is calculated from barley areas under specific input types, provided by the International Food Policy Research Institute (IFPRI) Spatial Production Allocation Model reported[30]. Yield is the reported yield at year around 2000[57].

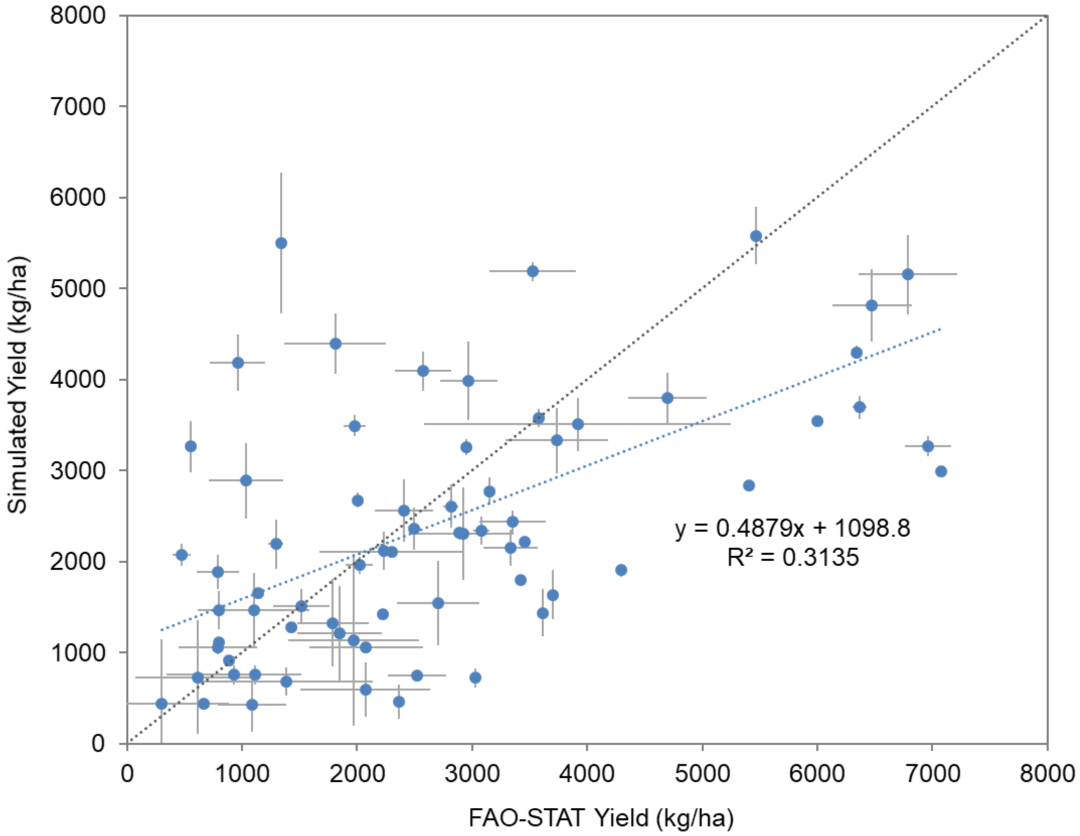


**Figure SI-17. FAO-STAT and Simulated National Barley Yields (n=102 countries/regions), averaged for period of 1981-2010.** Error bar is the yearly variability of yield (n=30 years).

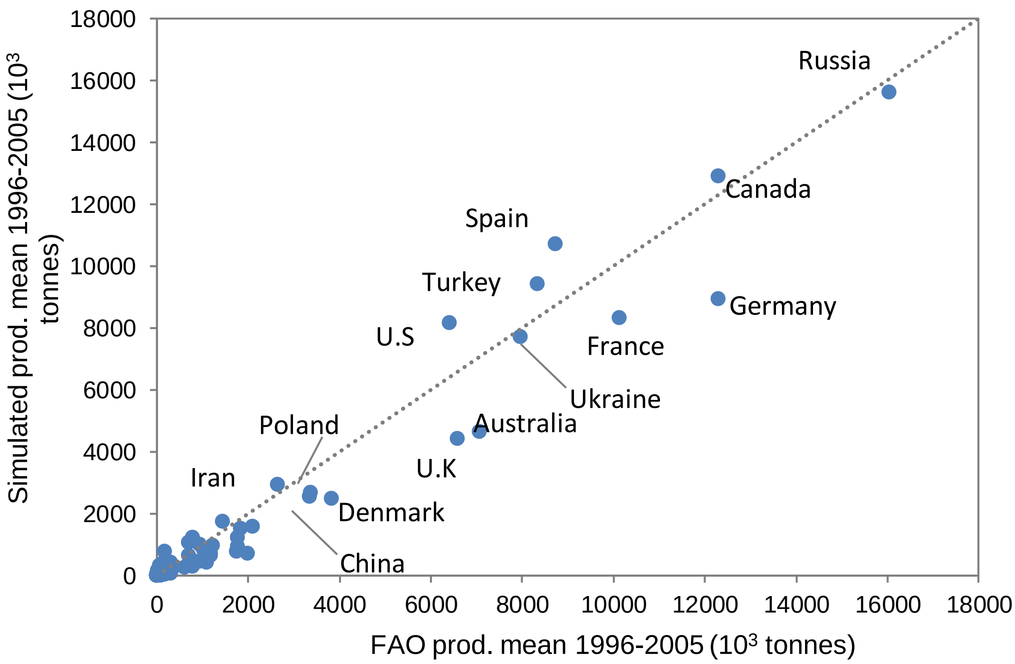


**Figure SI-18. FAO and Simulated National Barley Productions (n=102 countries/regions), averaged for period of 1996 to 2005.**

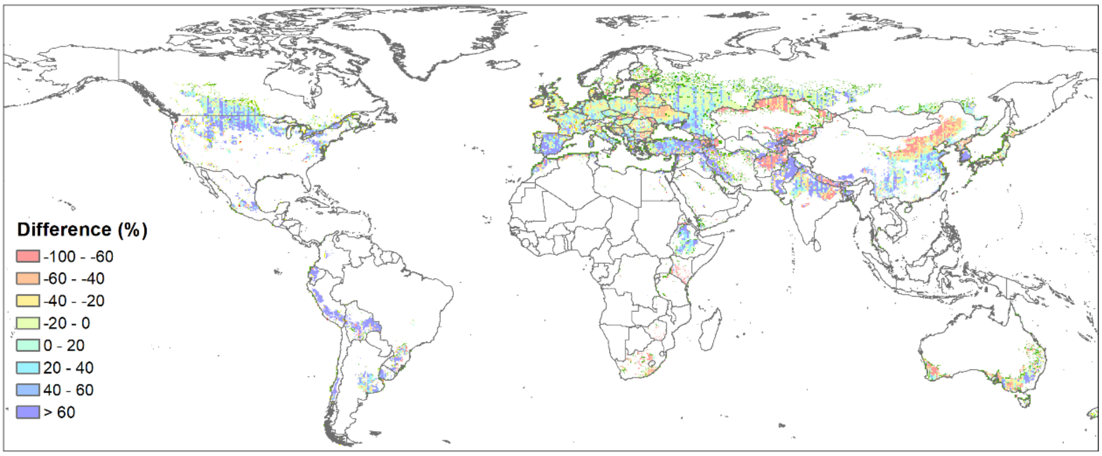


**Figure SI-19. Percentage difference of simulated yield to reported barley yield.** Simulated yield is mean from 1996 to 2005, while reported yield is from Monfreda et al.[57], representing the yield level of year 2000.

### 3.2.2 Projection of future barley yield change compared with recent yield

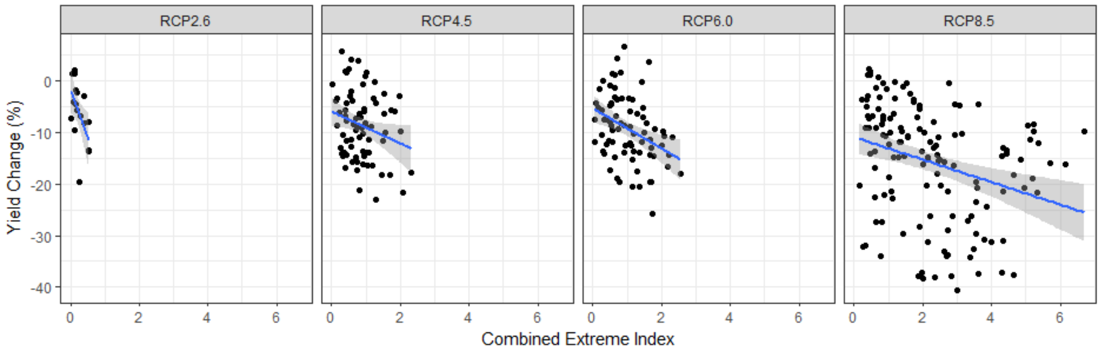


**Figure SI-20. Relationships between Yield Change and Combined Extreme Index under the Emission Pathways.** Blue line denotes linear regression line with 95% confidence interval (n=17, 77, 80, and 139 of extreme events in RCP2.6, RCP4.5, RCP6.0, and RCP8.5, respectively).

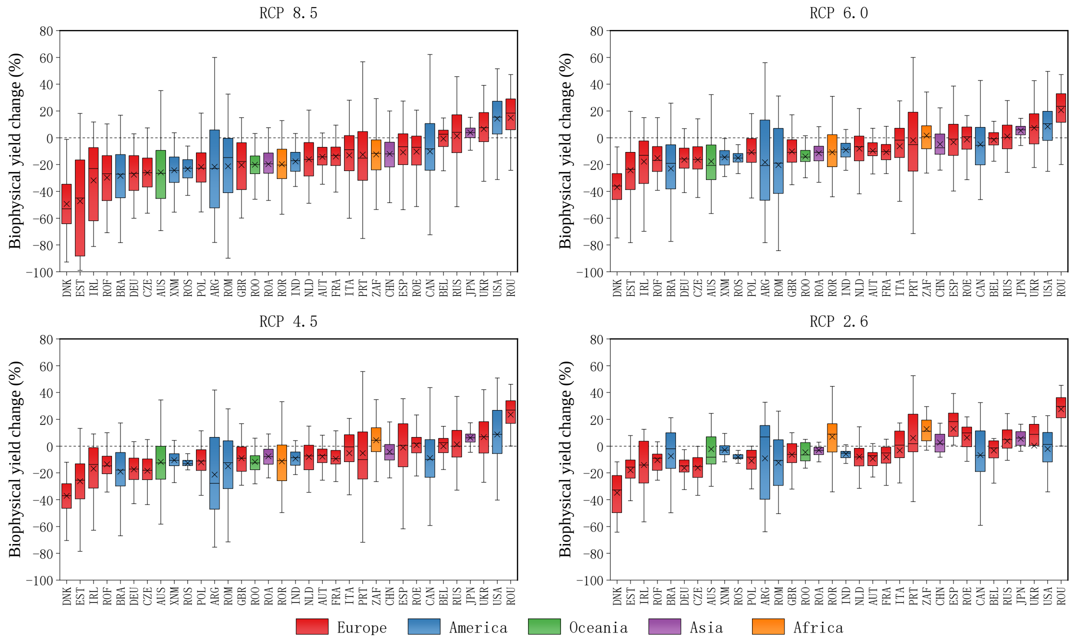


**Figure SI-21. Biophysical yield change (%)** (Top and bottom of the boxes are 25th and 75th percentiles, and the centerline is the 50th of the data. Two whiskers indicate the minimum and maximum of all data - n=17, 77, 80, and 139 of extreme events in RCP2.6, RCP4.5, RCP6.0, and RCP8.5, respectively; The countries/regions' ordering is from most severe to least severe effects in RCP8.5 and then for the other RCPs the order is preserved. The corresponding full names for three letter country/region acronyms are given in Appendix Table A2.)

### 3.3 The impacts of extreme events on barley supply

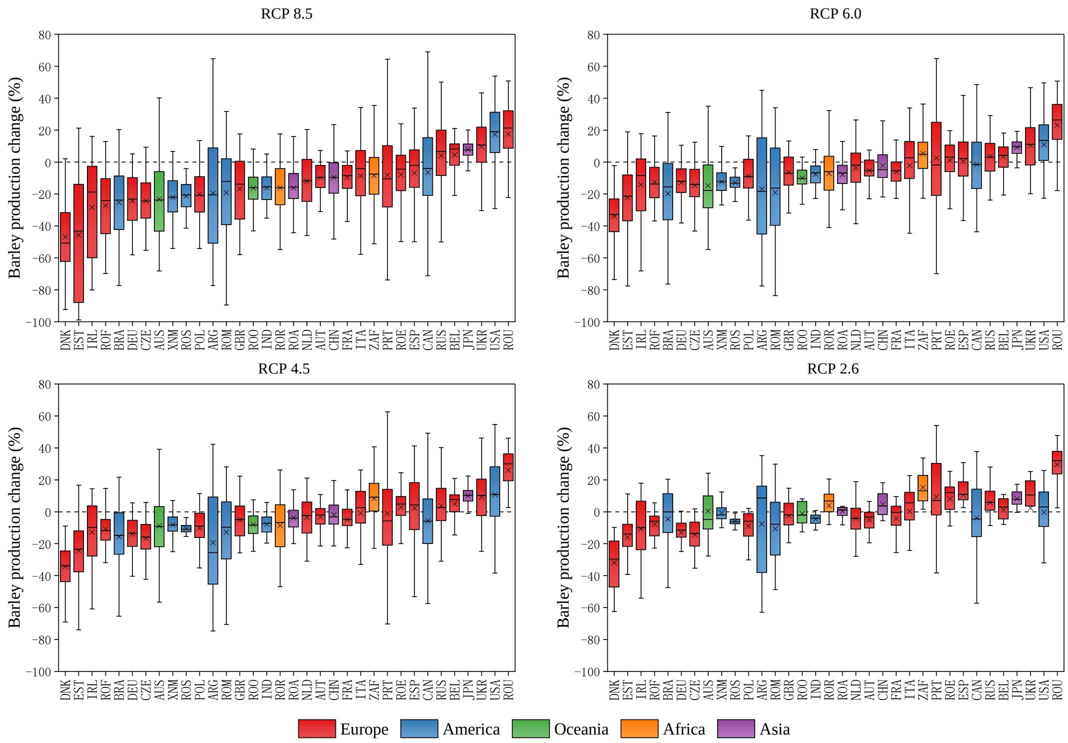


**Figure SI-22. Barley production change during extreme events (%).** (Top and bottom of the box are 25th and 75th percentiles, and the centerline is the 50th of the data. Two whiskers indicate the minimum and maximum of all data - n=17, 77, 80, and 139 of extreme events in RCP2.6, RCP4.5, RCP6.0, and RCP8.5, respectively; The countries/regions' ordering is from most severe to least severe effects in RCP8.5 and then for the other RCPs the order is preserved. The corresponding full names for three letter country/region acronyms are given in Appendix Table A2.)

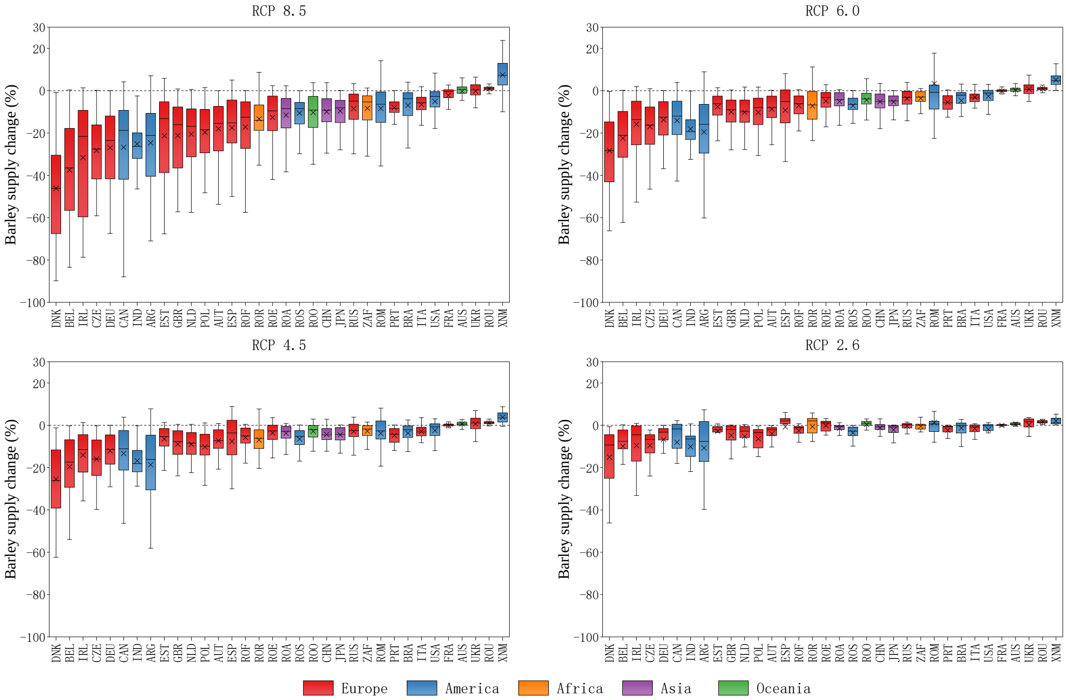


**Figure SI-23. Barley supply change during extreme events (%).** (Top and bottom of the box are 25th and 75th percentiles, and the centerline is the 50th of the data. Two whiskers indicate the minimum and maximum of all data - n=17, 77, 80, and 139 of extreme events in RCP2.6, RCP4.5, RCP6.0, and RCP8.5, respectively; The countries/regions' ordering is from most severe to least severe effects in RCP8.5 and then for the other RCPs the order is preserved. The corresponding full names for three letter country/region acronyms are given in Appendix Table A2.)

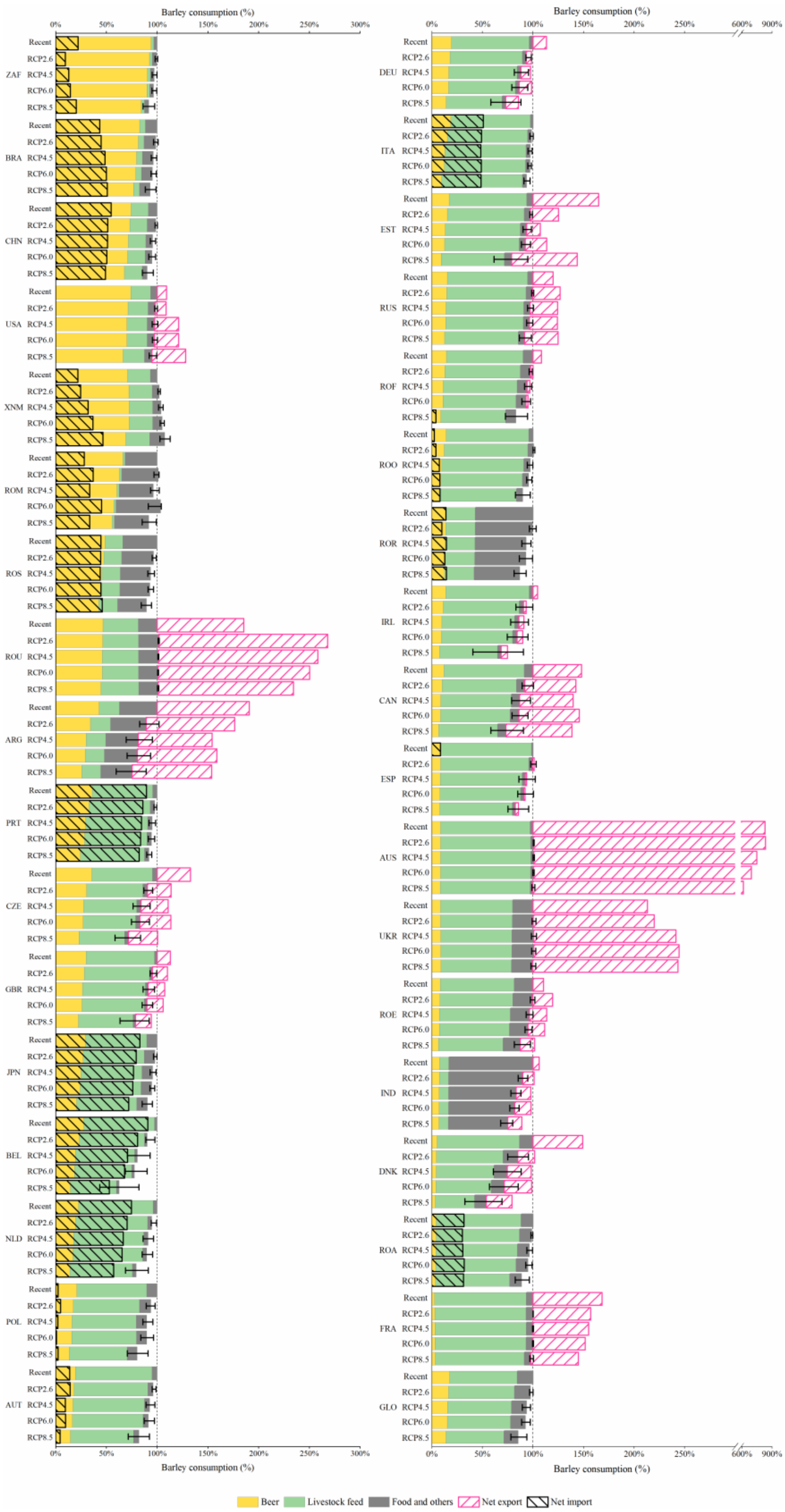


**Figure SI-24. 'Absolute' barley share to different uses for all countries/regions (%), the total beer consumption under RCPs reflects the changes to recent levels** (Two whiskers indicate 25th and 75th percentiles of all data - n=17, 77, 80, and 139 of extreme events in RCP2.6, RCP4.5, RCP6.0, and RCP8.5, respectively. The corresponding full names for three letter country/region acronyms are given in Appendix Table A2.)

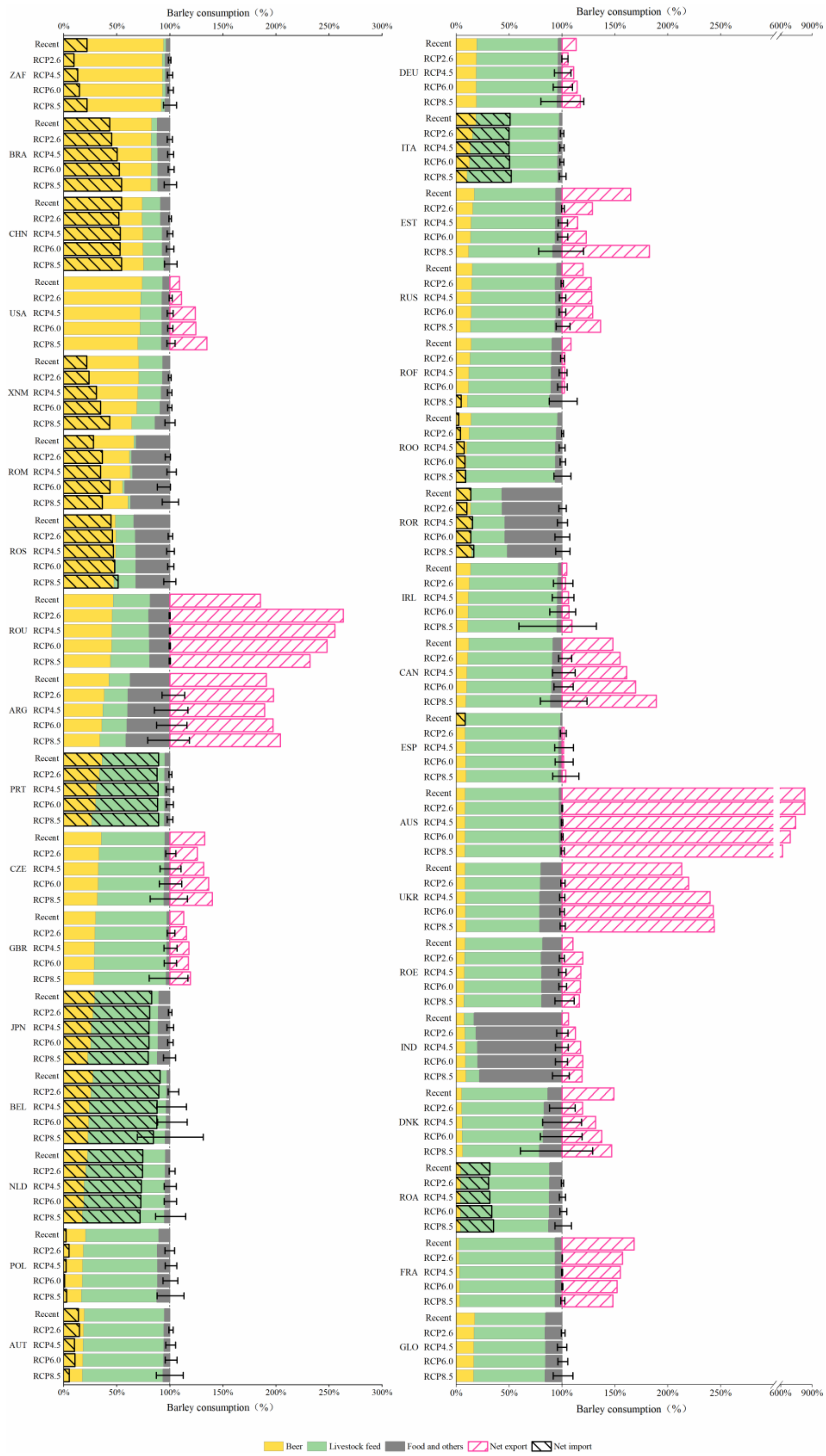


**Figure SI-25. 'Relative' barley share to different uses for all countries/regions (%), the total beer consumption under all scenarios are 100** (Two whiskers indicate 25th and 75th percentiles of all data - n=17, 77, 80, and 139 of extreme events in RCP2.6, RCP4.5, RCP6.0, and RCP8.5, respectively. The corresponding full names for three letter country/region acronyms are given in Appendix Table A2.)

### 3.4 The impacts of extreme events on beer supply and price

All the regions/countries included in the model have some production, trade, and different use of barley. However, for some countries, like India, due to consumer preference or some cultural factors, the per capita or total beer consumptions are quite low. We believe that presenting the beer consumption and/or price changes for such countries are not of much interest. Also, for the regional aggregations, although we have the results for their beer consumption changes but we cannot compare beer price changes for these regions due to unavailability of a region-wise representative base price. Therefore, here we only present the changes in beer consumption and beer price for the main beer consuming countries (defined in terms of either total beer consumption or per capita beer consumption ranked in top 50% of the countries in our economic model), which altogether account for 73% of the countries covered in our economic model (See Figs. SI-25 for the main beer consuming countries).

#### 3.4.1 Percent changes of beer production, consumption and price

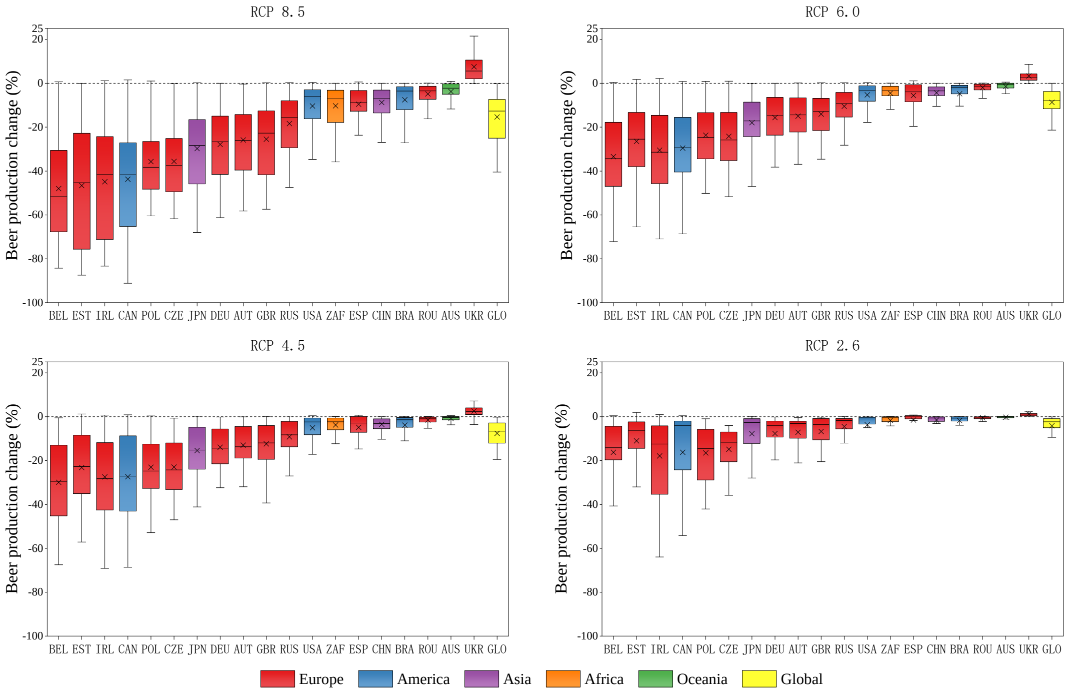


**Figure SI-26. Beer production change for the main beer consuming countries (%)** (Top and bottom of the box are 25th and 75th percentiles, and the centerline is the 50th of the data. Two whiskers indicate the minimum and maximum of all data-n=17, 77, 80, and 139 of extreme events in RCP2.6, RCP4.5, RCP6.0, and RCP8.5, respectively; The countries/regions' ordering is from most severe to least severe effects in RCP8.5 and then for the other RCPs the order is preserved. The corresponding full names for three letter country/region acronyms are given in App. Table A2.)

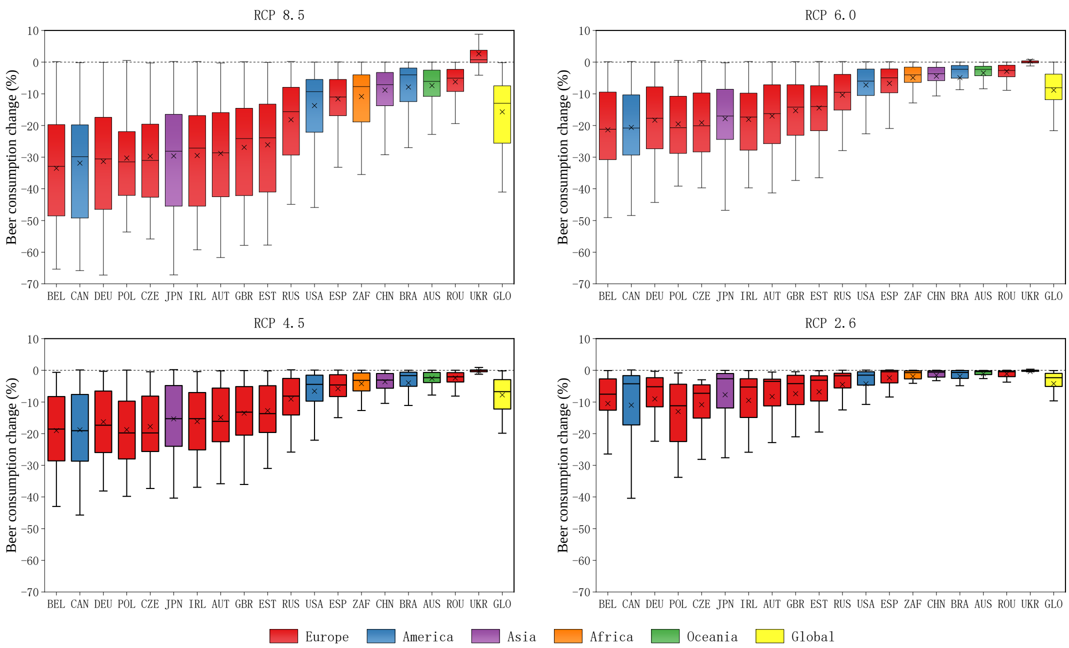


**Figure SI-27. Beer consumption change for the main beer consuming countries (%)** (Top and bottom of the box are 25th and 75th percentiles, and the centerline is the 50th of the data. Two whiskers indicate the minimum and maximum of all data - n=17, 77, 80, and 139 of extreme events in RCP2.6, RCP4.5, RCP6.0, and RCP8.5, respectively; The countries/regions' ordering is from most severe to least severe effects in RCP8.5 and then for the other RCPs the order is preserved. The corresponding full names for three letter country/region acronyms are given in App. Table A2.)

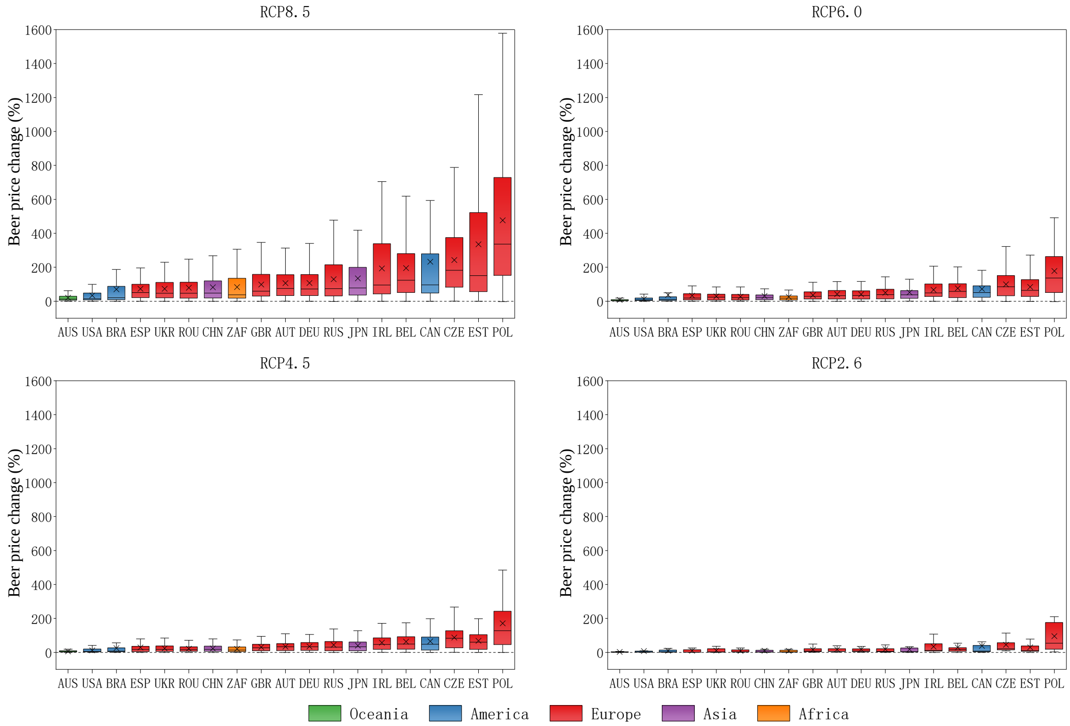


**Figure SI-28. Percent change in beer price for the main beer consuming countries** (Top and bottom of the box are 25th and 75th percentiles, and the centerline is the 50th of the data. Two whiskers indicate the minimum and maximum of all data - n=17, 77, 80, and 139 of extreme events in RCP2.6, RCP4.5, RCP6.0, and RCP8.5, respectively; The countries/regions' ordering is from lowest to highest price increase in RCP8.5 and then for the other RCPs the order is preserved. The corresponding full names for three letter country/region acronyms are given in App. Table A2.)

### 3.4.2 Absolute changes of barley production, total/per capita beer consumption and price

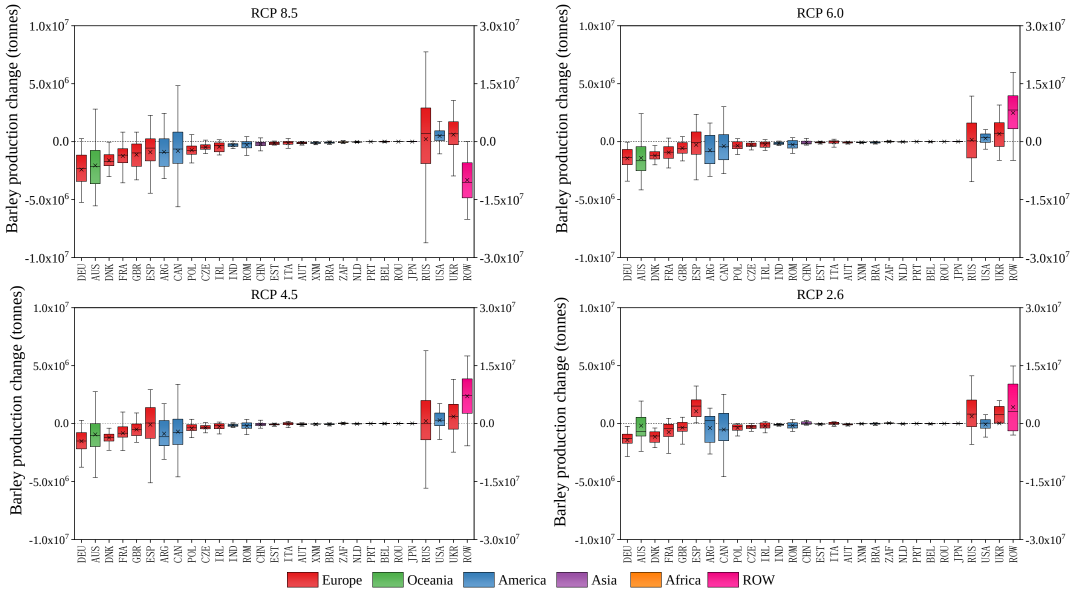


**Figure SI-29. Barley production change for the countries/regions (metric tons)** (Top and bottom of the box are 25th and 75th percentiles, and the centerline is the 50th of the data. Two whiskers indicate the minimum and maximum of all data - n=17, 77, 80, and 139 of extreme events in RCP2.6, RCP4.5, RCP6.0, and RCP8.5, respectively; The countries/regions' ordering is from most severe to least severe effects in RCP8.5 and then for the other RCPs the order is preserved. The corresponding full names for three letter country/region acronyms are given in App. Table A2.)

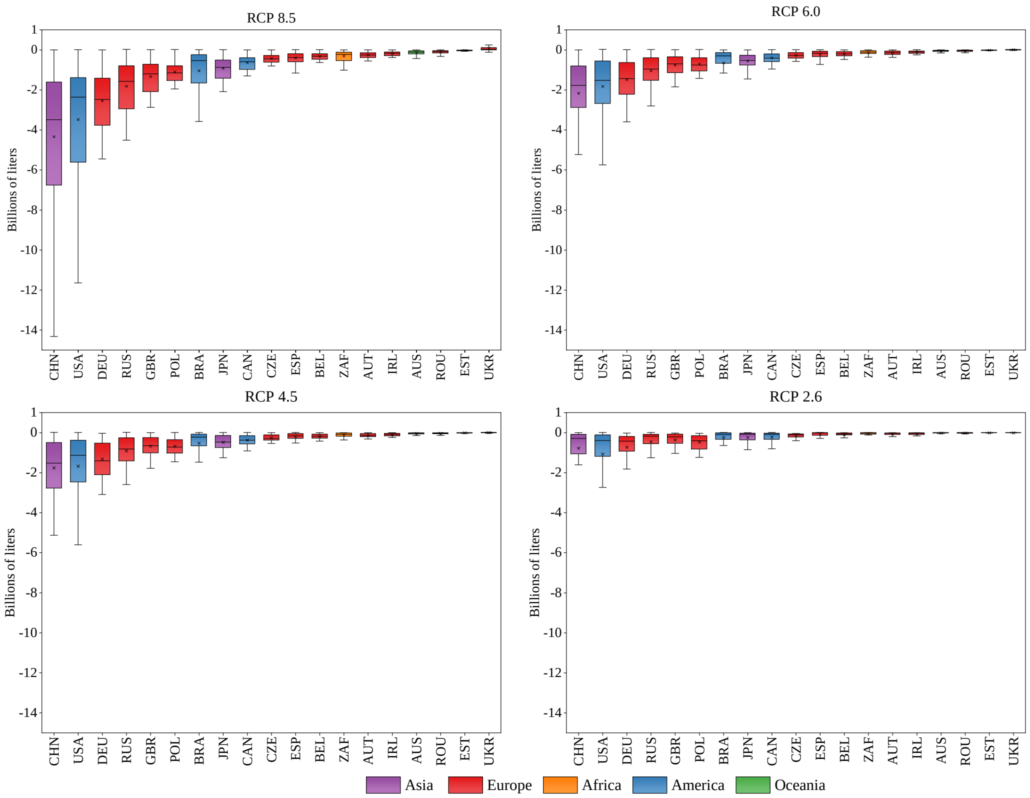


**Figure SI-30. Total beer consumption changes for the main beer consuming countries (billions of litters)** (Top and bottom of the box are 25th and 75th percentiles, and the centerline is the 50th of the data. Two whiskers indicate the minimum and maximum of all data - n=17, 77, 80, and 139 of extreme events in RCP2.6, RCP4.5, RCP6.0, and RCP8.5, respectively; The countries/regions' ordering is from most severe to least severe effects in RCP8.5 and then for the other RCPs the order is preserved. The corresponding full names for three letter country/region acronyms are given in Appendix Table A2.)

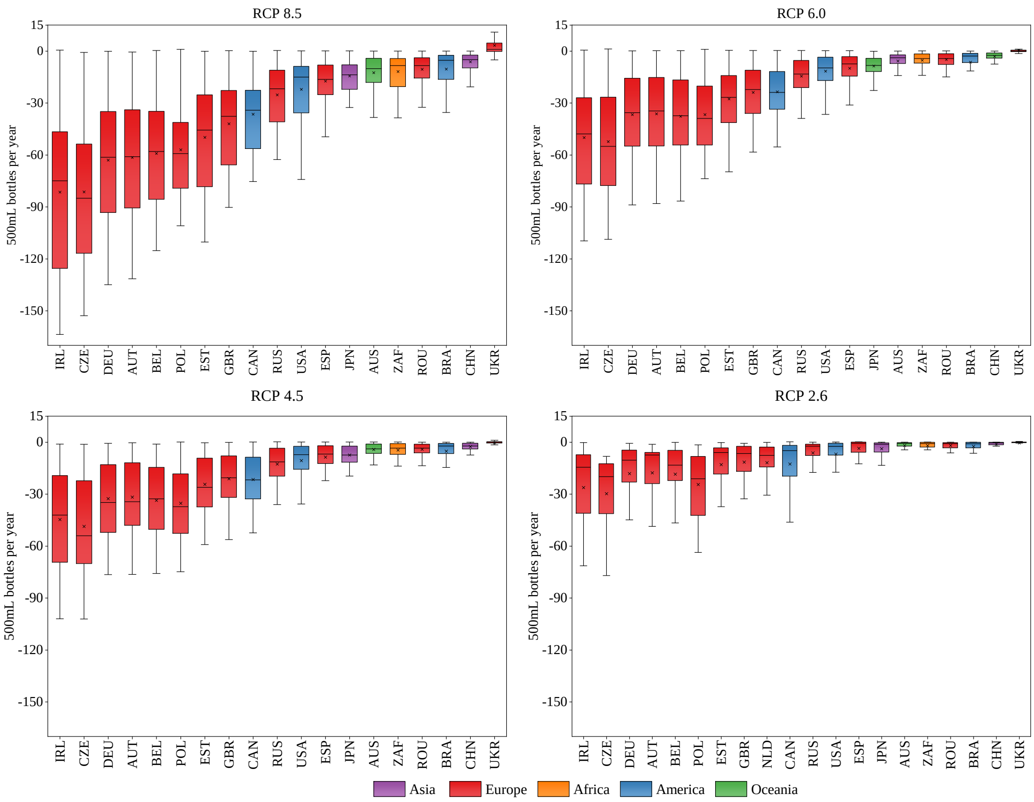


**Figure SI-31. Per capita beer consumption change for the main beer consuming countries (500 mL bottles per year)** (Top and bottom of the box are 25th and 75th percentiles, and the centerline is the 50th of the data. Two whiskers indicate the minimum and maximum of all data - n=17, 77, 80, and 139 of extreme events in RCP2.6, RCP4.5, RCP6.0, and RCP8.5, respectively; The countries/regions' ordering is from most severe to least severe effects in RCP8.5 and then for the other RCPs the order is preserved. The corresponding full names for three letter country/region acronyms are given in Appendix Table A2.)

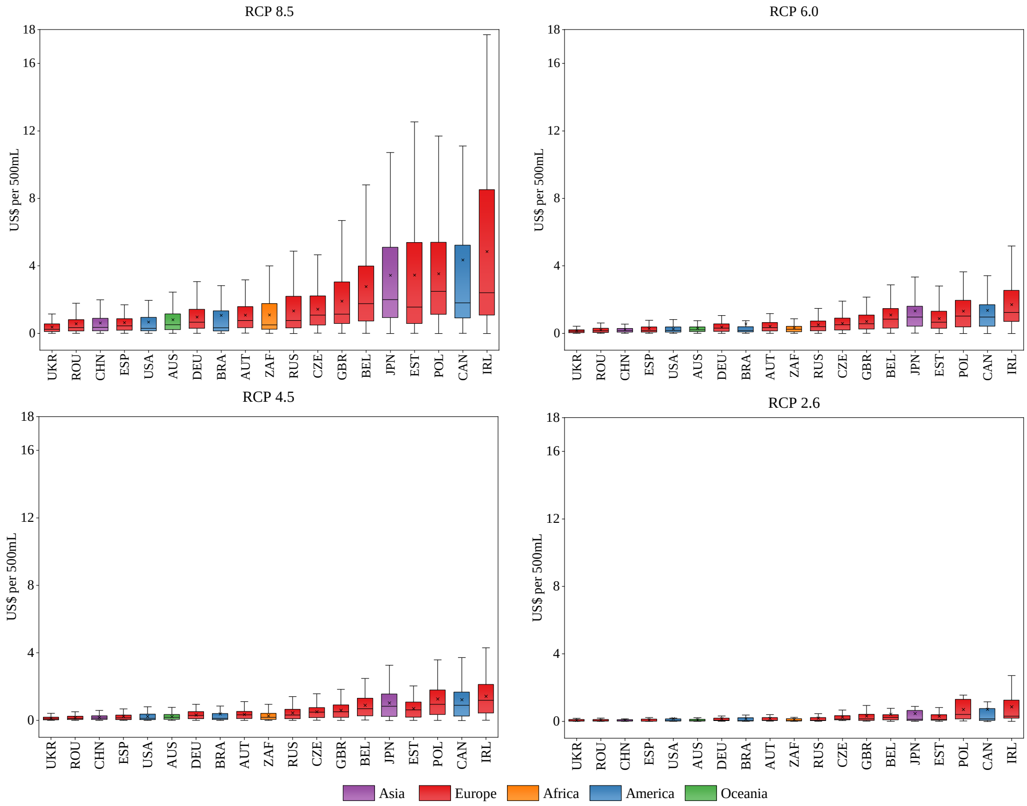


**Figure SI-32. Beer price change (US$ per 500mL) for the main beer consuming countries** (Top and bottom of the box are 25th and 75th percentiles, and the centerline is the 50th of the data. Two whiskers indicate the minimum and maximum of all data - n=17, 77, 80, and 139 of extreme events in RCP2.6, RCP4.5, RCP6.0, and RCP8.5, respectively; The countries/regions' ordering is from lowest to highest price increase in RCP8.5 and then for the other RCPs the order is preserved. The corresponding full names for three letter country/region acronyms are given in App. Table A2.)

## 3.5 Comparison between mean climate changes' impacts and extreme events' impacts

### 3.5.1 Barley yield changes

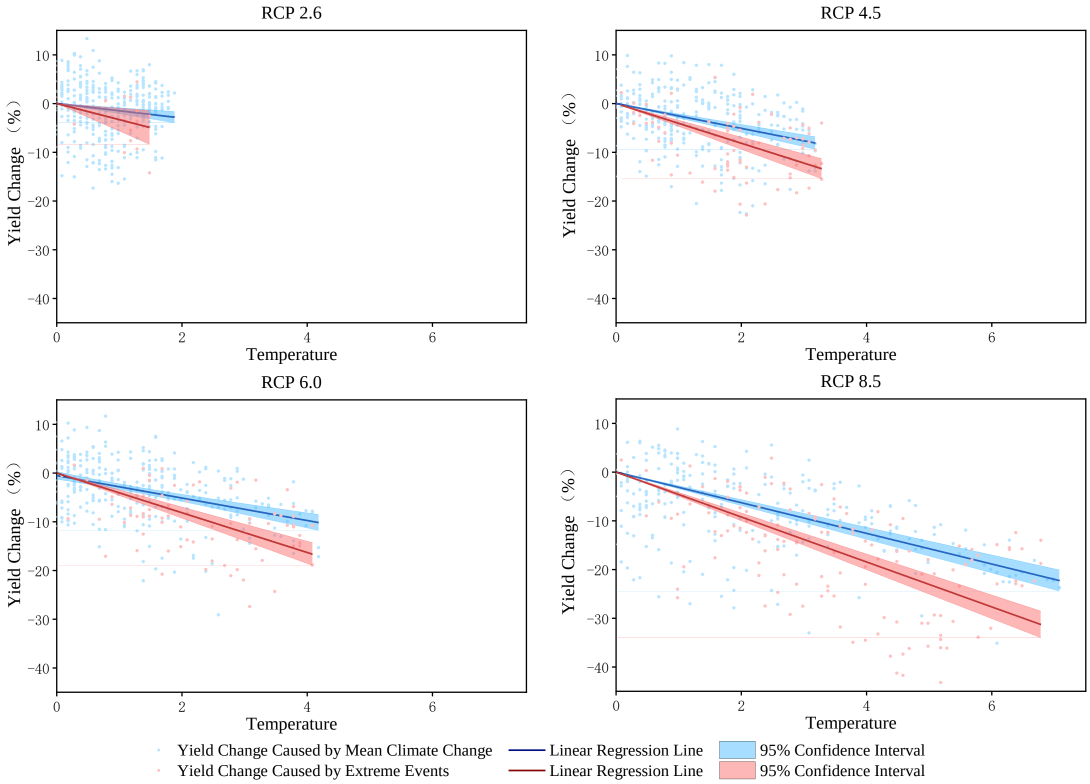


**Figure SI-33. Global barley yield changes with temperature increase under mean climate change and extreme events (%).** n=450 mean climate changes for each RCP; n=17, 77, 80, and 139 of extreme events in RCP2.6, RCP4.5, RCP6.0, and RCP8.5, respectively.

Fig. SI-33 shows that as the temperature increases, the impacts of extreme events on barley yield become larger than the impacts of mean climate change under all RCPs. The uncertainty (measured by confidence interval) of the impacts caused by extreme events is also higher than the mean climate change. For example, under RCP8.5, the impacts caused by extreme events are two times the impacts caused by mean climate change at the end of this century. It is noted that these are the average impacts at global level; if we focus on certain countries or regions, the difference can be more obvious. The study, therefore, assesses the worst impacts from extreme events and considers that adaptation can cope with the impacts from mean climate change to some extent but would fail to cover the losses from extreme events.

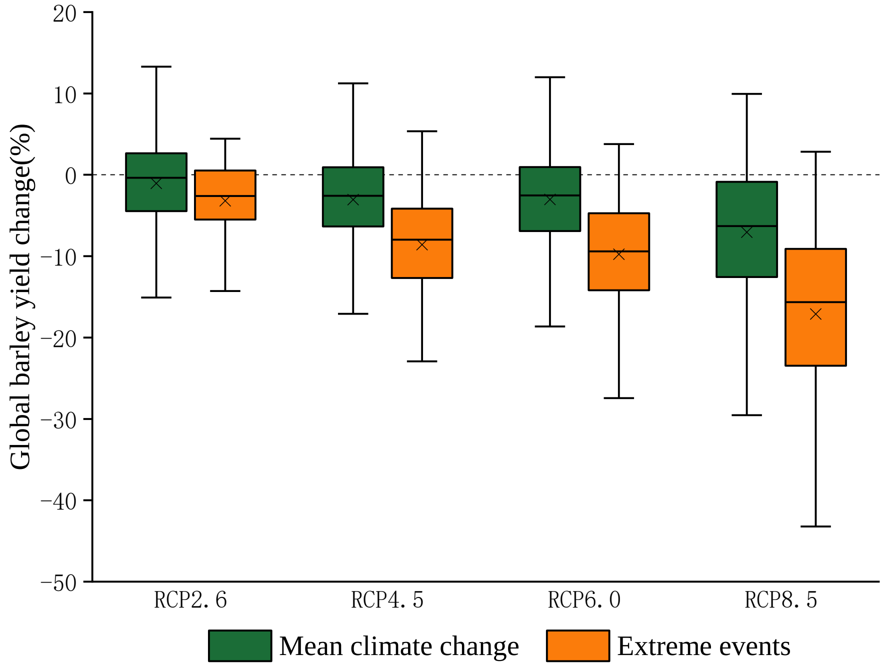


**Figure SI-34. Global barley yield changes under mean climate change and extreme events (%).** (Top and bottom of the box are 25th and 75th percentiles, and the centerline is the 50th of the data. Two whiskers indicate the minimum and maximum of all data - n=450 mean climate changes for each RCP; n=17, 77, 80, and 139 of extreme events in RCP2.6, RCP4.5, RCP6.0, and RCP8.5, respectively.)

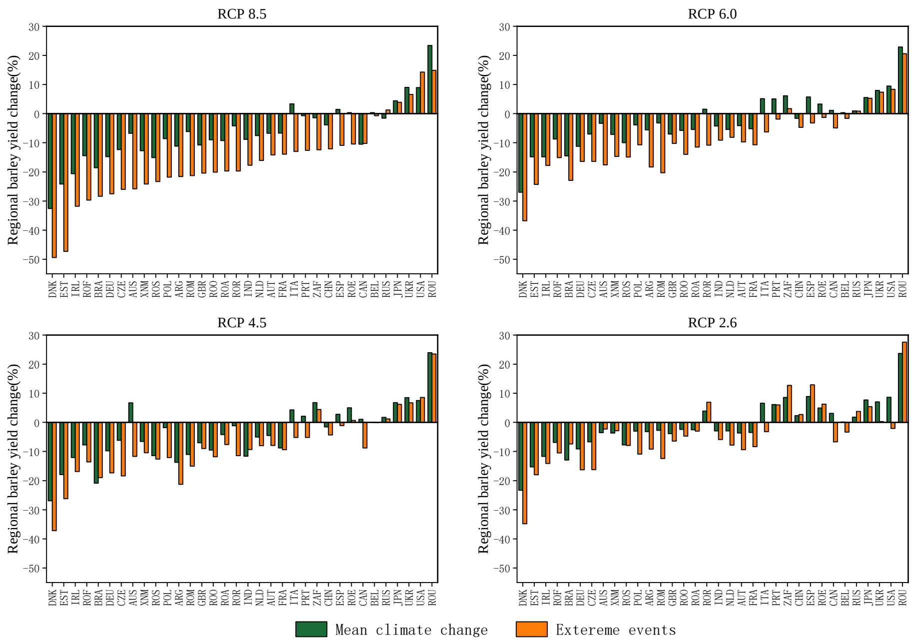


**Figure SI-35. Barley yield changes in all countries/regions under mean climate change and extreme events, average impacts during 2010-2099 (%)** (The countries/regions' ordering is from most severe to least severe effects of extreme events in RCP8.5 and then for the other RCPs the order is preserved. The corresponding full names for three letter country/region acronyms are given in App. Table A2.)

### 3.5.2 Beer consumption changes

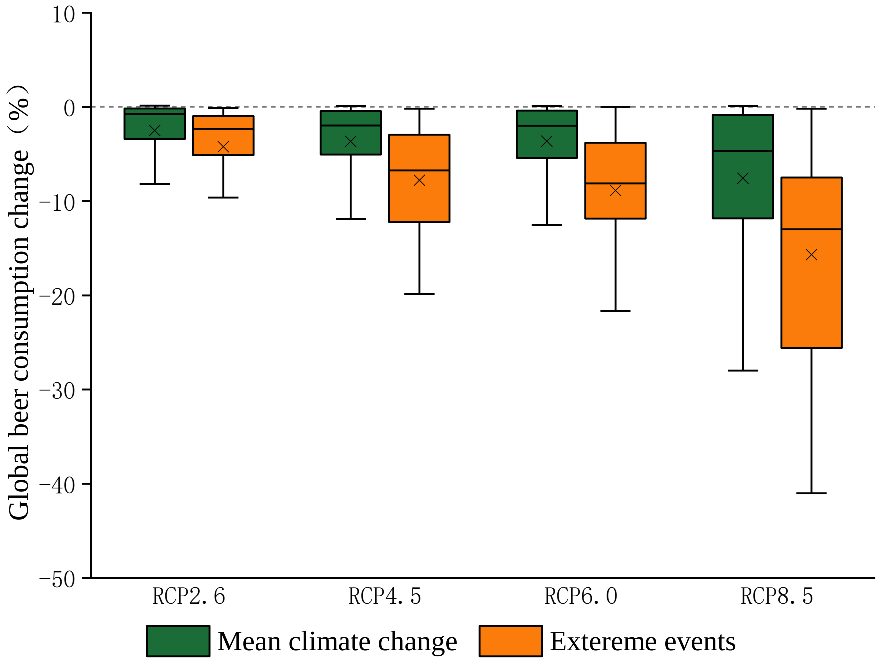


**Figure SI-36. Global beer consumption changes under mean climate change and extreme events (%).** (Top and bottom of the box are 25th and 75th percentiles, and the centerline is the 50th of the data. Two whiskers indicate the minimum and maximum of all data - n=450 mean climate changes for each RCP; n=17, 77, 80, and 139 of extreme events in RCP2.6, RCP4.5, RCP6.0, and RCP8.5, respectively.)

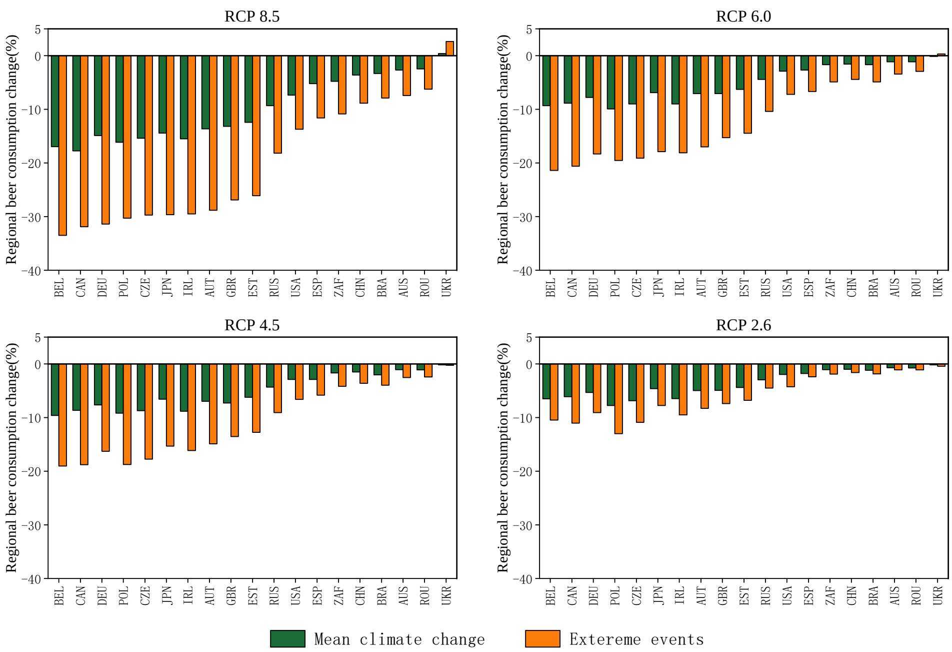


**Figure SI-37. Beer consumption changes in all countries/regions under mean climate change and extreme events, average impacts during 2010-2099 (%).** (The countries/regions' ordering is from most severe to least severe effects of extreme events in RCP8.5 and then for the other RCPs the order is preserved. The corresponding full names for three letter country/region acronyms are given in Appendix Table A2.bbb)

### 3.6 Uncertainty and limitations

We decompose the uncertainty into contributions of "physical shocks" uncertainty, "technology" uncertainty, and "economic behavior" uncertainty. The uncertainty is identified by changing single input one at a time (with ±10% variation) while holding the other inputs at their original values[56]. "Reported estimation" refer to the original average impacts on beer consumption during 2010-2099; "Physical shocks" uncertainty comes from the physical models and possible barley stockpiling by changing the barley yield shock size; "Technology" uncertainty comes from better/worse technology that can lower/increase the amount of barley required to produce the same quantity beer; "Economic behavior" uncertainty comes from the possible changes of the parameter related to beer price elasticity, the parameter related to income elasticity and the ease of substitution of land with other inputs for barley production (further decomposed in Fig. SI-39 below); "Interaction" uncertainty is the residual when all factors are sampled simultaneously. We compare the contributions of the above sources of uncertainty (mean absolute uncertainty of ±10% variation) based on the "reported estimation" that refer to the original average impacts on beer consumption during 2010-2099. Figs. SI-38 and SI-39 show that technology has major impacts on the results. The second major uncertainty comes from physical shocks. Regarding economic behaviors, beer price elasticity has more obvious impacts than other economic factors.

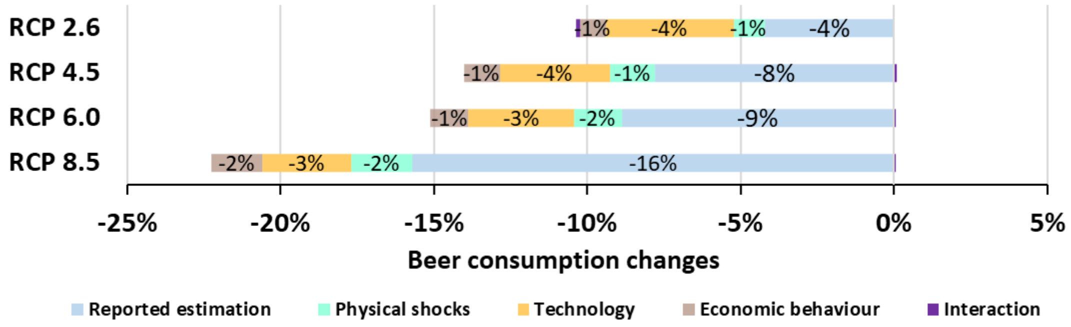


**Figure SI-38. Decomposing sources of uncertainty for average beer consumption changes**

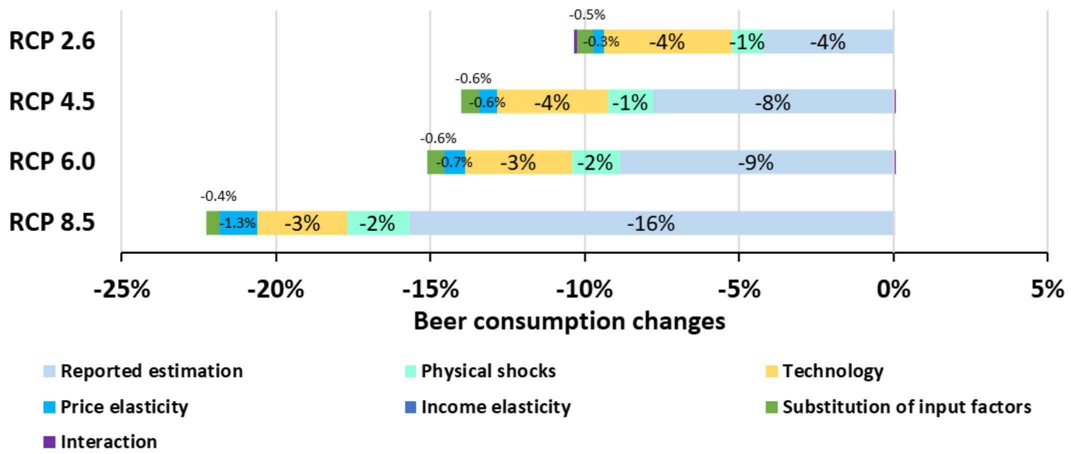


**Figure SI-39. Decomposing sources of uncertainty from economic behaviors and other factors for average beer consumption changes**

Although we analyze different sources of uncertainty, our methodological approach in this study has some important limitations deserving discussion, including our use of a single crop model to estimate barley yields, and the fact that our estimates of impact are based on the current agricultural practices, global economy, population, and prevailing dietary/beverage preferences.

A single crop model (DSSAT) is used to evaluate the effects of drought and heat on barley yields. The DSSAT model is known to underestimate yield damages caused by spikelet sterility and leaf senescence under droughts and heatwaves[58,59], and to neglect the possibility that pest and disease attacks could also happen concurrently[60]. The model runs do not include $CO_2$ fertilization or $CO_2$-induced changes in water use efficiency, although the beneficial effects of such changes may be limited under drought conditions[61]. Despite these limitations, numerous studies demonstrate model skill in reproducing historical barley yields[14-18], and a Europe-focused model intercomparison shows that yields projected by the DSSAT model are near the mean of nine crop models[19].

Our results reflect impacts of extreme events as though they happened in today's world. For example, we do not assess the effects of potential future changes in barley agriculture, such as increases in farm productivity due to new technology; the use of different, more drought- or heat-tolerant barley cultivars; or increases in barley stockpiling (we presented a review of challenges of stockpiling barley for beer in SI section 2.4). Similarly, global population and socio-economic conditions are held constant. Further studies may incorporate these factors for a more complete picture of beer supply in the future; as a first step, we seek to isolate the effects of extreme climatic events holding all other conditions constant.

Especially the expected changes in cultivated crop in the years following a disaster would possibly affect the results greatly. As we are unaware of any previous analyses on this topic, we have examined the question ourselves. We focused on whether a correlation exists between barley yield in a given year and barley harvested area in the following year, performing historical analyses using time series data between 1961-2016 from the FAOSTAT[1] to look at the major production anomalies (> 10% yield loss), following the approach below:

1. In each country, we first detrended the barley yield data using a simple linear regression and subtracting off the trend line.
2. Then we detrended data for each country's barley area similarly.
3. We compared the yield anomalies for country-years with large yield reductions (> 10% decline relative to the previous year). Yield in each year (t) is compared with harvested area anomalies in the next year (t+1), i.e. to see whether a negative yield shock in 1990 lead to less or more barley area in 1991.
4. We also considered normalizing all the yields and area anomalies by subtracting off the mean and scaling using the standard deviation. In this way, it is easier to compare all the countries together in a graph (Fig. SI-40).

We used two-sided t test as significance test. The results are presented in Table SI-2 and Fig. SI-40, below. The results for detrended data show no significant relationship between a given year's yield change and next year's harvested area for barley. The results for normalized series show significant but a very weak negative effect of yield changes on barley area in t+1 year, suggesting that farmers would increase their barley cultivation by small amount following a disaster year. Given that both methods show different (significant and insignificant) results, we cannot be certain about the existence (or lack thereof) of a relationship between reduction in barley yield and change in harvested area during the next year. So in our simulation, we do not consider the area change impacts.

**Table SI-2. Relationship between barley yield and harvested area (with year-on-year yield change <-10%)**

| VARIABLES | (1) Area detrended $_t$ | (2) Area standard $_t$ |
|---|---|---|
| **Yield detrended$_{t-1}$** | 2.139 | |
| | (2.151) | |
| **Yield standard $_{t-1}$** | | -0.0645*** |
| | | (0.0188) |
| **Constant** | 9,733 | 0.00577 |
| | (9,270) | (0.0199) |
| **Observations** | 2,900 | 2,424 |
| **R-squared** | 0.000 | 0.005 |
| **Number of area code** | 113 | 113 |

Standard errors in parentheses
*** p<0.01, ** p<0.05, * p<0.1

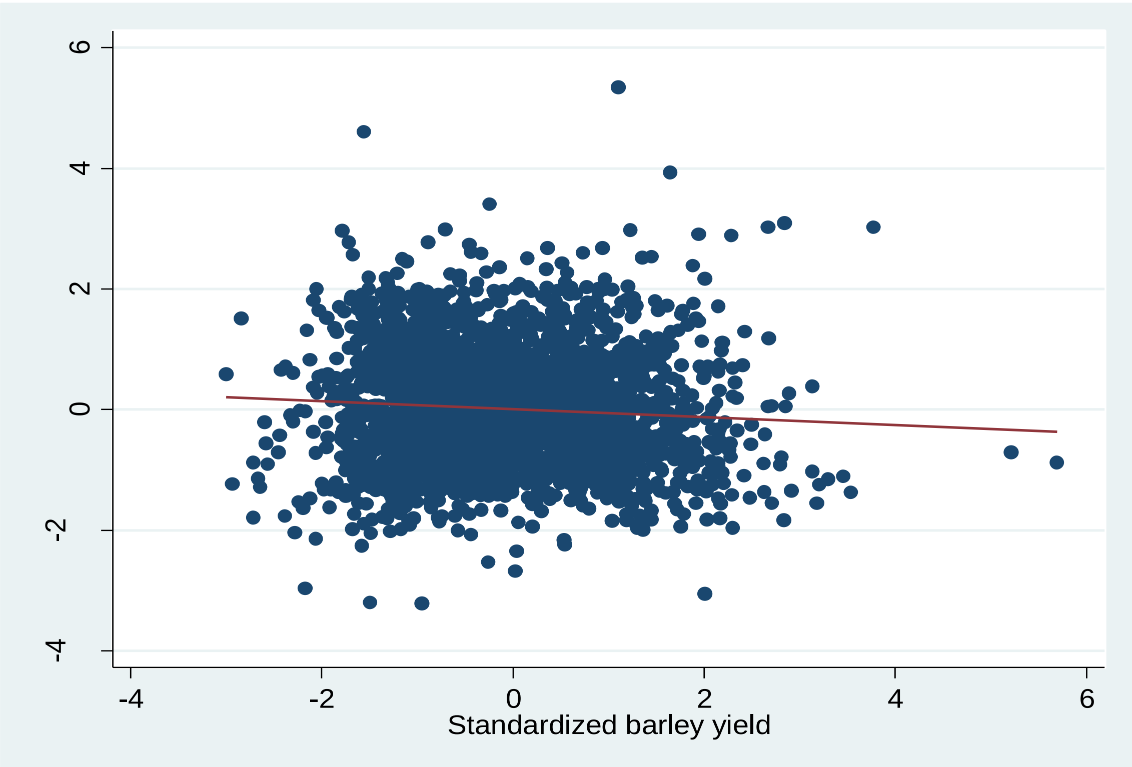


**Figure SI-40. Scatter gram between standardized yield and standardized harvested area of barley (with year-on-year yield change <-10%)** (n=2424 independent experiments)

**Reference:**


1 FAOSTAT, 2017. (FAOSTAT online database, 1981-2010, 2011, 2017) http://www.fao.org/faostat/en/#data.

2 McKee, T. B., Doesken, N. J. & Kleist, J. The Relationship of Drought Frequency and Duration to Timescales. (Eighth Conference on Applied Climatology, 1993)

3 Sacks, W.J., Deryng, D., Foley, J.A. & Ramankutty, N. Crop planting dates: an analysis of global patterns. *Glob. Ecol. Biogeo.* 19, 607-620 (2010).

4 Ruane, A.C., Goldberg, R., & Chryssanthacopoulos, J. Climate forcing datasets for agricultural modeling: Merged products for gap-filling and historical climate series estimation. *Agr. & Forest Meteorol.* 200, 233-248 (2015).

5 Guttman, N. B. Accepting the standardized precipitation index: a calculation algorithm. Journal of the American Water Resources Association 35(2), 311-322 (1999).

6 Lobell, D. & Gourdji, S. The Influence of Climate Change on Global Crop Productivity. Plant Physiology 160, 1686–1697 (2012).

7 Lobell, D.B., Hammer, G.L., McLean, G., Messina, C., Roberts, M.J. & Schlenker, W. The critical role of extreme heat for maize production in the United States. Nature Climate Change 3, 497–501 (2013).

8 Sakata, T., Takahashi, H., Nishiyama, I. Effects of High Temperature on the Development of Pollen Mother Cells and Microspores in Barley Hordeum vulgare L. Journal of Plant Research 113(4), 395-402 (2000).

9 Abiko, M., Akibayashi, K., Sakata, T., et al. High-temperature induction of male sterility during barley (Hordeum vulgare L.) anther development is mediated by transcriptional inhibition. Sexual Plant Reproduction 18(2), 91-100 (2005).

10 Oshino, T., Abiko, M., Saito, R., et al. Premature progression of anther early developmental programs accompanied by comprehensive alterations in transcription during high-temperature injury in barley plants. Molecular Genetics & Genomics 278(1), 31-42 (2007).

11 Hempel, S., Frieler, K., Warszawski L., Schewe, J., & Piontek, F. A trend-preserving bias correction – the ISI-MIP approach. *Earth Syst. Dynam. Discuss.* 4, 219-236 (2013).

12 Thorp, K.R., DeJonge, K.C., Kaleita, A.L., Batchelor, W.D. & Paz, J.O. Methodology for the use of DSSAT models for precision agriculture decision support. *Comput. & Electron. in Agri.* 64, 276-285 (2008).

13 Gbegbelegbe, S. et al. Baseline simulation for global wheat production with CIMMYT mega-environment specific cultivar. *Field Crops Res.* 202, 122-135 (2017).

14 Trnka, M., Dubrovsky, M., & Zalud, Z. Climate change impacts and adaptation strategies in spring barley production in the Czech Republic. Clim. Chang. 64, 227-255 (2004).

15 Travasso, M. I., & Magrin, G. O. Utility of CERES-Barley under Argentine condition. Field Crops Research 57, 329-333 (1998).

16 Hlavinka, P. et al. The performance of CERES-Barley and CERES-Wheat under various soil conditions and tillage practices in Central Europe. Die Bodenkultur 61(1), 5-16 (2010).

17 Holden, N. M., Brereton, A. J., Fealy, R., & Sweeney, J. Possible change in Irish climate and its impact on barley and potato yields. Agri Forest Meteorol. 116, 181-196 (2003).

18 Fatemi, R. Z., Paknejad, F., Amiri, E., Nabi, I. M., & Mehdi, M. S. Investigation of barley productivity responses to different water consumption by using the CERES-Barley model. J. Biol. Environ. Sci. 9(27), 119-126 (2015).

19 Rotter, R. P. et al. Simulation of spring barley yield in different climatic zones of Northern and Central Europe: A comparison of nine crop models. Field Crop Research 133, 23-26 (2012).

20 Hoogenboom, G. *et al.* Decision Support System for Agrotechnology Transfer (DSSAT) Version 4.6 (http://dssat.net). DSSAT Foundation, Prosser, Washington (2015).

21 Elliott, J. et al. Constraints and potentials of future irrigation water availability on agricultural production under climate change. *Proc. Natl Acad. Sci. USA* 111, 3239-3244 (2014).

22 Elliott, J. et al. The Global Gridded Crop Model intercomparison: data and modeling protocols for Phase I (v1.0). *Geosci. Model Dev. Discuss.* 7, 4383-4427 (2014).

23 Mueller, N. D. et al. Closing yield gaps through nutrient and water management. Nature 490, 254-257 (2012).

24 Naab, J.B., Boote, K.J., Jones, J.W. & Porter, C.H. Adapting and evaluating the CROPGRO-peanut model for response to phosphorus on a sandy-loam soil under semi-arid tropical conditions. *Field Crops Res.* 176, 71-86 (2015).

25 Dzotsi, K.A. et al. Modeling soil and plant phosphorus within DSSAT. *Ecol. Model.* 221, 2839-2849 (2010).

26 FAO/IIASA/ISRIC/ISSCAS/JRC, 2012. Harmonized World Soil Database, version 1.2. (FAO, Rome and IIASA, Luxemburg, Austria, 2012).

27 Xiong, W., Holman, I., Conway, D., Lin, E. & Li, Y. A crop model cross calibration for use in regional climate impact studies. *Ecol. Model.* 213, 365-380 (2008).

28 Xiong, W., Conway, D., Holman, I. & Lin, E. Evaluation of CERES-Wheat simulation of wheat production in China. *Agron. J.* 100, 1720-1728 (2008).

29 Xiong et al. Can climate-smart agriculture reverse the recent slowing of rice yield growth in China? Agriculture, Ecosystems & Environment 196, 125-136 (2014).

30 You, L. et al. Spatial production allocation model (SPAM) 2000, version 3 Release 2. http://MapSpam.info. (2009)

31 Schildbach, R. Centenary Review, Barley Worldwide. J Inst. Brew. 92, 11 (1986).

32 World Agricultural Outlook Board. 1994. Major World Crop Areas and Climatic Profiles. Agricultural Handbook No. 664. U.S. Department of Agriculture.

33 Rosenzweig, C. et al. Assessing agricultural risks of climate change in the 21st century in a global gridded crop model intercomparison. *Proc. Natl Acad. Sci. USA* 111, 3268-3273 (2014).

34 Rosenzweig, C. et al. The agricultural model intercomparison and improvement project (AgMIP): protocols and pilot studies. *Agr. & Forest Meteorol.* 170, 166-182 (2013).

35 Asseng, S. et al. Uncertainty in simulating wheat yields under climate change. *Nat. Clim. Change* 3, 827-832 (2013).

36 Bassu, S. et al. How do various maize crop models vary in their response to climate change factors? *Glob. Change Biol.* 20, 2301-2320 (2014).

37 Hertel, T.W. *Global Trade Analysis: Modeling and Applications*. (Cambridge Univ. Press, New York, 1997).

38 Corong, E. L., Hertel, T. W., McDougall, R., Tsigas, M. E. and van der Mensbrugghe, D. The Standard GTAP Model, Version 7. *J. of Glob. Econo. Analysis*. 2, (2017).

39 Ciscar, J.C. *et al.* Physical and economic consequences of climate change in Europe. *Proc. Natl Acad. Sci. USA* 108, 2678-2683 (2011).

40 Hsiang, S. *et al.* Estimating economic damage from climate change in the United States. *Science* 356, 1362–1369 (2017).

41 Taheripour, F., Hertel, T. W., and Liu, J. The role of irrigation in determining the global land use impacts of biofuels. *Energ. Sustain. & Soci.*3, (2013).

42 Ali, T., Huang, J.K. & Yang, J. Impact assessment of global and national biofuels developments on agriculture in Pakistan. *Appl. Energ.* 104, 466–474 (2013)

43 Yang, J., Huang, J.K., Qiu, H.G., Rozelle, S., & Sombilla, M. A. Biofuels and the greater Mekong Subregion: assessing the impact on prices, production and trade. *Appl. Energ.* 86, S37-S46 (2009).

44 Horridge, M. SplitCom, programs to disaggregate a GTAP sector. (Centre of Policy Studies, Monash University, 2005) http://www.monash.edu.au/policy/SplitCom.htm

45 DESA/UNSD, 2016. (United Nations Comtrade database, 2016) https://comtrade.un.org/data.

46 Nelson, J. P. Estimating the price elasticity of beer: Meta-analysis of data with heterogeneity, dependence, and publication bias. Journal of Health Economics. 33(1), 180-187 (2014).

47 Nelson, G.C. et al. Climate change effects on agriculture: Economic responses to biophysical shocks. Proc. Natl Acad. Sci. USA 111, 3274–3279(2014).

48 Palatnik, R. R. & Roson, R. Climate change and agriculture in computable general equilibrium models: alternative modeling strategies and data needs. Climatic Change 112, 1085-1100 (2012).

49 Iglesias, A., Garrote, L., Quiroga, S. & Moneo, M. A regional comparison of the effects of climate change on agricultural crops in Europe. Climatic Change 112, 29-46 (2012).

50 Rose, A., & Liao, S. Modeling regional economic resilience to disasters: a computable general equilibrium analysis of water service disruptions. J. of Reg. Sci. 45, 75–112 (2005).

51 Rose, A., Oladosu, G. & Liao, S.Y. Business interruption impacts of a terrorist attack on the electric power system of Los Angeles: Customer resilience to a total blackout. Risk Analysis 27, 513–531 (2007)

52 USDA, 2017. (United States Department of Agriculture, National Agricultural Statistics Service, 2017) https://quickstats.nass.usda.gov/

53 White, N.G.G., Hulasare, R.B. & Jayas, D.S. Effect of storage conditions on quality loss of hull-less and hulled oats and barley. Canadian Journal of Plant Science 79, 475–482 (1999).

54 Woods, J.L., Favier, J.F. &Briggs, D.E. Predicting the germinative energy of dormant malting barley during storage. Journal of the Institute of Brewing 100, 257–269 (1994).

55 FAO, Division, F. I. C. Agribusiness handbook: Barley, Malt, Beer. (FAO, 2009).

56 Hawkins, E., Sutton, R. The potential to narrow uncertainty in regional climate predictions. Bull. Am. Meteorol. Soc. 90, 1095–1107 (2009). doi:10.1175/2009BAMS2607.1

57 Monfreda, C., Ramankutty, N., & Foley, J. A. Farming the planet: 2. Geographic distribution of crop areas, yields, physiological types, and net primary production in year 2000, Glob. Biogeochem. Cycles 22, GB1022 (2008).

58 Liu, B. et al. Testing the responses of four wheat crop models to heat stress at anthesis and grain filling. Global Change Biology 22, 1890-1903 (2016).

59 Otter-Nacke S. J., Ritchie, J. T, Godwin, D., Singh, U. A User's Guide to CERES Barley-V2.10. International Fertilizer Development Centre. Muscle Shoals, AL. USA (1991).

60 Elad, Y. & Pertot, I. Climate Change Impacts on Plant Pathogens and Plant Diseases. Journal of Crop Improvement 28, 99-139 (2014).

61 Gray, S. et al. Intensifying drought eliminates the expected benefits of elevated carbon dioxide for soybean. Nature Plants 2, 1-8 (2016)

## Appendix Tables

**Table A1. Sectoral aggregation scheme**

| **Aggregated sectors** | **GTAP original sectors** |
|---|---|
| Barley | Split from the original “other grains” sector |
| Beer | Split from the original “beverage and tobacco” sector |
| Trade | Trade |
| Recreational services | Recreational services |
| Other beverage and tobacco | Beverage and tobacco after splitting out beer |
| Wheat | Wheat |
| Other grains | Cereal grains nec. after splitting out barely |
| Rice | Paddy rice; Processed rice |
| Edible oils | Oil seeds; Vegetable oils and fats |
| Cotton | Plant-based fibers |
| Other agriculture | Sugar cane, sugar beet; Vegetables, fruit, nuts; Crops nec; Forestry; |
| Livestock | Bovine cattle, sheep and goats, horses; Animal products nec; Raw milk; Wool, silk-worm cocoons; Fishing; Bovine meat products; Meat products nec; Dairy products; |
| Processed food | Sugar; Food products nec |
| Energy | Coal; Oil; Gas; Petroleum, coal products ; Electricity; Gas manufacture, distribution |
| Extraction | Minerals nec; Mineral products nec; Ferrous metals; Metals nec; Metal products |
| Light manufacturing | Textiles; Wearing apparel; Leather products; Wood products; Paper products, publishing; Chemical, rubber, plastic products; Motor vehicles and parts; Manufactures nec |
| Heavy manufacturing | Transport equipment nec; Electronic equipment; Machinery and equipment nec |
| Transportation & communication | Transport nec; Water transport; Air transport; Communication |
| Other Services | Water; Construction; Financial services nec; Insurance; Business services nec; Public Administration, Defense, Education, Health; Dwellings; |

**Table A2. Regions aggregation scheme**

| Aggregated regions | Short name | GTAP original regions |
|---|---|---|
| Australia | AUS | Australia |
| Rest of Oceania | ROO | New Zealand, Rest of Oceania |
| China | CHN | China |
| Japan | JPN | Japan |
| Rest of Asia | ROA | Hong Kong, South Korea, Mongolia, Taiwan, Republic of China, Rest of East Asia , Brunei Darussalam , Cambodia , Indonesia , Laos , Malaysia, Philippines , Singapore, Thailand, Vietnam, Rest of Southeast Asia, Bangladesh, Nepal, Pakistan, Sri Lanka, Rest of South Asia, Kazakhstan, Kyrgyzstan, Rest of Former Soviet Union, Armenia, Azerbaijan, Georgia, Bahrain, Iran, Israel, Jordan, Kuwait, Oman, Qatar, Saudi Arabia, Turkey, United Arab Emirates, Rest of Western Asia |
| India | IND | India |
| Canada | CAN | Canada |
| United States of America | USA | United States of America |
| Rest of North America | XNM | Mexico, Rest of North America |
| Argentina | ARG | Argentina |
| Brazil | BRA | Brazil |
| Rest of South America | ROS | Bolivia, Chile, Colombia, Ecuador, Paraguay, Peru, Uruguay, Venezuela, Rest of South America |
| Rest of America | ROM | Costa Rica, Guatemala, Honduras, Nicaragua, Panama, El Salvador, Rest of Central America, Dominican Republic, Jamaica, Puerto Rico, Trinidad and Tobago, Caribbean |
| Austria | AUT | Austria |
| Belgium | BEL | Belgium |
| Czech Republic | CZE | Czech Republic |
| Denmark | DNK | Denmark |
| Estonia | EST | Estonia |
| France | FRA | France |
| Germany | DEU | Germany |
| Ireland | IRL | Ireland |
| Italy | ITA | Italy |
| Netherlands | NLD | Netherlands |
| Poland | POL | Poland |
| Portugal | PRT | Portugal |
| Spain | ESP | Spain |
| Great Britain | GBR | Great Britain |
| Rest of EFTA | ROF | Cyprus, Finland, Greece, Hungary, Latvia, Lithuania, Luxembourg, |

| | | |
|---|---|---|
| | | Malta, Slovakia, Slovenia, Sweden, Switzerland, Norway, Rest of EFTA |
| Romania | ROU | Romania |
| Russian Federation | RUS | Russian Federation |
| Ukraine | UKR | Ukraine |
| Rest of Europe | ROE | Albania, Bulgaria, Belarus, Croatia, Rest of Eastern Europe, Rest of Europe |
| South Africa | ZAF | South Africa |
| Rest of Africa | ROR | Egypt, Morocco, Tunisia, Rest of North Africa, Benin, Burkina Faso, Cameroon, Cote d'Ivoire, Ghana, Guinea, Nigeria, Senegal, Togo, Rest of Western Africa, Central Africa, South Central Africa, Ethiopia, Kenya, Madagascar, Malawi, Mauritius, Mozambique, Rwanda, Tanzania, Uganda, Zambia, Zimbabwe, Rest of Eastern Africa, Botswana, Namibia, Rest of South African Customs Union, Rest of the World |